

RENIERAMYCIN T DERIVATIVE DH_22 INDUCES APOPTOSIS IN LUNG CANCER CELLS BY
DOWNREGULATION OF C-MYC PROTEIN



A Thesis Submitted in Partial Fulfillment of the Requirements
for the Degree of Master of Science in Pharmaceutical Sciences and Technology

FACULTY OF PHARMACEUTICAL SCIENCES

Chulalongkorn University

Academic Year 2022

Copyright of Chulalongkorn University

อนุพันธ์ของเรเนียร์รามัยซิน ที ดีเอช₂
เหนี่ยวนำการตายแบบอะพอพโทซิสในเซลล์มะเร็งปอดโดยการลดลงของโปรตีน C-Myc



วิทยานิพนธ์นี้เป็นส่วนหนึ่งของการศึกษาตามหลักสูตรปริญญาวิทยาศาสตรมหาบัณฑิต
สาขาวิชาเภสัชศาสตร์และเทคโนโลยี ไม่สังกัดภาควิชา/เทียบเท่า
คณะเภสัชศาสตร์ จุฬาลงกรณ์มหาวิทยาลัย
ปีการศึกษา 2565
ลิขสิทธิ์ของจุฬาลงกรณ์มหาวิทยาลัย

อินเดียนา กีตา อังเกรนิ : อนุพันธ์ของเรเนียร์รามัยซิน ที ดีเอช_22

เหนี่ยวนำการตายแบบอะพอพโทซิสในเซลล์มะเร็งปอดโดยการลดลงของโปรตีน C-Myc.

(RENIERAMYCIN T DERIVATIVE DH_22 INDUCES APOPTOSIS IN LUNG

CANCER CELLS BY DOWNREGULATION OF C-MYC PROTEIN) อ.ที่ปรึกษาหลัก :

ศ. ภก. ดร.ปิติ จันทร์วรโชติ

มะเร็งปอดเป็นสาเหตุการตายที่แพร่หลาย ซึ่งระบุได้จากระดับ c-Myc ที่สูงขึ้น เราสังเคราะห์อนุพันธ์ใหม่ของ renieramycin T (RT) ชื่อ DH_22 และทดสอบฤทธิ์ต้านมะเร็งในเซลล์มะเร็งปอดของมนุษย์ ในการทดสอบความมีชีวิตของเซลล์และการทดสอบการย้อมสีด้วยนิวเคลียส พบว่า DH_22 เป็นพิษต่อเซลล์ โดยมี IC50 ประมาณ 13 ไมโครโมลาร์ ; และพบว่าช่วยใกล้เคียงการตายของเซลล์มะเร็งปอด ในขณะเดียวกัน ในแง่กลไก DH_22 มีส่วนในการเปิดใช้งานของ apoptosis ที่ขึ้นกับ p53 และลดระดับเซลล์ของ c-Myc กลไกที่ขึ้นกับ p53 ถูกกระตุ้นโดยการเพิ่มขึ้นของ p53 การเหนี่ยวนำของโปรตีน Bax ที่ก่อการตายของเซลล์และการลดลงของโปรตีน B-cell lymphoma 2 (Bcl-2) ที่ต่อต้าน apoptotic ความเข้มของการเรืองแสงของ Akt, p-Akt และ c-Myc ก็ลดลงอย่างมากเช่นกัน ตรวจพบ Akt และ p-Akt ในไซโตพลาสซึมและนิวเคลียส ในขณะที่ c-Myc ส่วนใหญ่อยู่ในนิวเคลียสของเซลล์ควบคุมที่ไม่ผ่านการบำบัด ผลลัพธ์เหล่านี้แสดงให้เห็นว่า DH_22 สามารถลด c-Myc ซึ่งสนับสนุนโดยการเชื่อมต่อระดับโมเลกุล กลไกการออกฤทธิ์ของ renieramycin T อนุพันธ์ DH_22 เริ่มต้นด้วยการยับยั้ง mTOR ซึ่งลดฟอสโฟริเลชันของ Akt ซึ่งลดฟอสโฟริเลชันของ GSK3b และเร่งการย่อยสลายของ c-Myc นอกจากนี้ DH_22 เองยังสามารถยับยั้ง Akt ผ่านการยับยั้ง allosteric ซึ่งอาจรบกวนการคงตัวของ c-Myc

สาขาวิชา เภสัชศาสตร์และเทคโนโลยี

ลายมือชื่อนิสิต

ปีการศึกษา 2565

ลายมือชื่อ อ.ที่ปรึกษาหลัก

6372014333 : MAJOR PHARMACEUTICAL SCIENCES AND TECHNOLOGY

KEYWORD: DH_22, Lung cancer, Apoptosis, p-Akt, c-Myc

Indiana Gita Anggraeni : RENIERAMYCIN T DERIVATIVE DH_22 INDUCES APOPTOSIS IN LUNG CANCER CELLS BY DOWNREGULATION OF C-MYC PROTEIN. Advisor: Prof. PITHI CHANVORACHOTE, Ph.D.

Lung cancer is a prevalent cause of death, indicated by an elevated c-Myc level. We synthesized a new derivative of renieramyacin T (RT), named DH_22, and tested it for anti-cancer activities in human lung cancer cells. In the cell viability and nuclear staining tests, DH_22 was discovered to be cytotoxic, with an IC_{50} of around 13 μM ; and found to mediate apoptosis in the lung cancer cells. Meanwhile, in a mechanistic sense, DH_22 contributed to the activation of p53-dependent apoptosis and decreased the cellular level of c-Myc. The p53-dependent mechanism was indicated by an increase of p53, an induction of the pro-apoptotic Bax protein, and a decrease of the anti-apoptotic B-cell lymphoma 2 (Bcl-2) protein. The fluorescence intensity of Akt, p-Akt, and c-Myc also declined significantly. Akt and p-Akt were detected in the cytoplasm and nucleus, while most of c-Myc was located in the nucleus of the untreated control cells. These results demonstrated that DH_22 could reduce c-Myc, supported by molecular docking. The mechanism of action of renieramyacin T derivative DH_22 starts with the inhibition of mTOR, which reduces the phosphorylation of Akt, which then reduces the phosphorylation of GSK3b and accelerates the degradation of c-Myc. In addition, DH_22 itself could inhibit Akt via allosteric inhibition, which could disrupt the c-Myc stabilization.

จุฬาลงกรณ์มหาวิทยาลัย
CHULALONGKORN UNIVERSITY

Field of Study: Pharmaceutical Sciences and Technology Student's Signature

Academic Year: 2022 Advisor's Signature

ACKNOWLEDGEMENTS

My utmost gratitude goes to my adviser, Professor Pithi Chanvorachote, Ph.D., who guided me through this research with skill and whose guidance has been very helpful. This study could not have been completed without his clear direction and unwavering support. His empathetic guidance and suggestions provide me with strength and confidence throughout my academic career.

My gratitude also goes to the thesis committee members: Assoc. Prof. Chatchai Chaotam, Ph.D., Asst. Prof. Wanatchaporn Arunmanee, Ph.D., and Sudjit Luanpitpong, Ph.D., for offering the guidelines and suggestions in this thesis.

I would like to thank the seniors of the physiology laboratory, who taught me useful techniques while conducting cell-based assays, as well as all the members of the Department of Pharmacology and Physiology, Faculty of Pharmaceutical Sciences, Chulalongkorn University, for valuable moments and a wonderful atmosphere.

I am extremely grateful to Chulalongkorn University for providing the Scholarship for International Graduate Students in ASEAN countries for my master's degree, as well as to The Education and Cultural Attaché of the Embassy of the Republic of Indonesia in Bangkok, who actively facilitates and provides opportunities outside of academic activities.

Above ground, I am profoundly grateful to my family for their love, support, and refusal to let me give up. Lastly, I would want to express my sincere appreciation to all of my friends who constantly contribute support and positive value. Without them, it would not have been feasible for me to accomplish my goal.

จุฬาลงกรณ์มหาวิทยาลัย
CHULALONGKORN UNIVERSITY

Indiana Gita Anggraeni

TABLE OF CONTENTS

	Page
ABSTRACT (THAI).....	iii
ABSTRACT (ENGLISH).....	iv
ACKNOWLEDGEMENTS	v
TABLE OF CONTENTS	vi
LIST OF TABLES	ix
LIST OF FIGURES	x
CHAPTER I.....	1
INTRODUCTION.....	1
1.1 Background and Rational.....	1
1.2 Objective.....	3
1.3 Hypothesis	3
1.4 Expected Benefit	3
1.5 Conceptual Framework.....	4
1.6 Experimental Design	4
CHAPTER II.....	5
LITERATURE REVIEW	5
2.1 Lung Cancer.....	5
2.2 Apoptosis	8
2.2.1 p-Akt	11
2.2.2 c-Myc.....	12
2.3 Renieramycin T derivative DH_22.....	13

CHAPTER III	15
METHODOLOGY.....	15
3.1 Preparation of DH_22 Stock Solution.....	15
3.2 Cell Lines and Culture	15
3.3 Cytotoxicity Assay.....	15
3.4 Annexin V-FITC/PI Staining Apoptotic Assay	16
3.5 Nuclear Staining Assay (Hoechst33342/PI)	16
3.6 Western Blot Analysis	17
3.7 Proliferation Assay.....	17
3.8 Clonogenic Cell Survival Assay.....	18
3.9 Immunofluorescence	18
3.10 Molecular Docking	19
3.11 Statistical Analysis.....	19
CHAPTER IV	20
RESULTS	20
4.1 Cytotoxicity and Apoptosis-Inducing Effect of Renieramycin T Derivative DH_22	20
4.2 DH-22 therapy demonstrates apoptotic characteristics.....	21
4.3 Mechanism of action of DH-22 suppressing lung cancer and inducing apoptosis	23
4.4 Cell proliferation and survival effect of renieramycin T derivative DH_22	24
4.5 Inhibition of survival regulators by renieramycin T derivative DH_22 therapy... ..	25
4.6 Molecular Docking Simulation Demonstrates the Interaction of DH_22 with the Akt/c-Myc Proteins.....	29
CHAPTER V	32

DISCUSSION AND CONCLUSION 32

REFERENCES 37

VITA..... 48



LIST OF TABLES

	Page
Table 1. Docking results of DH_22.....	30



LIST OF FIGURES

	Page
Figure 1. Percentage of new cases and deaths from cancer worldwide in 2020 by different cancer types.....	5
Figure 2. Map showing estimated age-adjusted incidence rates for lung cancer globally in 2020 for both sexes and all ages.....	6
Figure 3. Intrinsic apoptosis pathway, internal cellular stress initiates the intrinsic pathway of apoptosis, also known as the mitochondrial pathway.	10
Figure 4. c-Myc signaling pathway, overexpression of c-Myc causes carcinogenesis, and it can be a potential target for anti-cancer treatment.	12
Figure 5. Structure of renieramycin T (RT) and renieramycin T derivative DH_22.	14
Figure 6. Synthesis of the renieramycin T derivative DH-22.....	20
Figure 7. Effect of DH-22 on cell viability and apoptotic cell death in the NSCLC cell line A549.....	21
Figure 8. Apoptotic characteristics of renieramycin T derivative DH_22 treatment....	22
Figure 9. The results of western blot analysis of several proteins.	23
Figure 10. DH_22 has a strong inhibitory effect on A549 cells.	25
Figure 11. Effect of DH_22 on Akt signaling pathway by immunofluorescence.....	26
Figure 12. Effect of DH_22 on GSK3 β altering c-Myc by immunofluorescence.....	28
Figure 13. Docking results of DH_22 on mTOR kinase domain of mTORC2 (PDB ID 4JT5).	30
Figure 14. Docking results of DH-22 on Akt1 (PDB ID 6S9W).	31
Figure 15. Proposed mechanism of action of DH_22.	36

CHAPTER I

INTRODUCTION

1.1 Background and Rational

Lung cancer cases have a high mortality rate, accounting for 2 million diagnoses and 1.8 million deaths worldwide (1). Molecular abnormalities are clearly associated with lung cancer development. One notable characteristic of cancer is the ability of tumor cells to evade apoptosis (2). Apoptosis, or programmed cell death, is triggered by intracellular signals. This process is crucial for cell homeostasis and elimination of cancer cells (3). Targeting apoptosis pathways has emerged as a promising strategy for cancer therapy. p53 is one of the genes that can initiate the apoptosis program. In response to DNA-damaging stimuli, p53 induces apoptosis or cell cycle arrest. p53 is the most comprehensively characterized tumor suppressor. This gene is frequently mutated in malignancies, inactivating the proapoptotic function of p53 and contributing to the drug-resistant phenotype (4).

p53 initiates responses such as cell cycle arrest, apoptosis, DNA repair, and cell differentiation by activating the transcription of specific target genes containing p53 DNA binding sites. Furthermore, the Bcl-2 protein family is one of the primary regulators of the mitochondria-mediated pathway to apoptosis. The mechanism of apoptosis may depend on p53, which stimulates the expression of several Bcl-2 family genes, including Bax. p53 can also bind to one or more anti-apoptotic mitochondrial proteins, such as Bcl-2, preventing the formation of the Bax mitochondrial pore and the subsequent release of cytochrome c (5) caspase activation and subsequently apoptotic cell death (6).

However, apoptosis resistance frequently occurs in cancer caused by the hyperactivation of survival pathways, including Akt (7) and c-Myc (8) facilitating cell growth, proliferation and angiogenesis (9). Akt, or Protein kinase B, is a serine/threonine-specific protein kinase activated by phosphorylation, an essential component of the PI3K/Akt signaling pathway. It triggers the development of

many human cancers and the formation of reactive oxygen species (10). Overexpression of p-Akt is directly correlated to the prognosis of hematologic and solid tumors such as squamous cell carcinoma (SCC) (11), gastric cancer (GC) (12), hepatocellular carcinoma (HCC) (13), ovarian cancer (OC) (14), and non-small cell lung cancer (NSCLC) (15, 16, 17, 18, 19).

Similarly, c-Myc, a proto-oncogene transcription factor, plays a key role in regulating other downstream signaling pathways and supports the development of a cell cycle, the metabolism of a cell for survival, and the activity of stem cells (20). Overexpression of the c-Myc protein often renders malignancies aggressive and resistant to treatment (21) as it induces the overactivation of stemness features. Recent studies have also demonstrated that c-Myc regulates other self-renewal transcription factors, boosting transcription and activities of these proteins (22, 23). It has been shown to be overexpressed in about 50-75% of NSCLC cases (24). An interaction between Akt and c-Myc is facilitated by protein stabilization (25). Akt stabilizes proteins, which allows the presence of c-Myc in cells. In other words, Akt protects the c-Myc protein from degradation (26), preventing it from destabilizing by inhibiting the phosphorylation at threonine 58 (Thr58). As a result, inhibiting p-Akt and c-Myc, which are located upstream and downstream of the signaling pathways, is a promising strategy.

Marine organisms offer biologically active compounds with the potential for new drug discovery (27). Renieramycin T (RT) is a tetrahydroisoquinoline alkaloid molecule isolated from the blue sponge *Xestospongia sp.* that has been pre-treated with potassium cyanide (28). Its anti-cancer properties have recently been examined in colon (HCT116), prostate (DU145) (29), non-small cell lung (H292, H460, and QG56) (30), breast (T47D), and pancreatic (AsPC1) cancer cells (28). However, despite the remarkable anti-cancer effects, the complex structure of RT makes large scale synthesis difficult. Accordingly, a simpler RT derivative, DH_22 compound, was synthesized and its anti-cancer activity was determined.

The discovery of DH_22 was primarily based on the presence of pyridine. The nucleus of pyridines is a well-studied six-membered heterocyclic moiety with a wide range of biological and medicinal applications (31, 32). With its established

anti-cancer property, pyridine is an impactful and valued moiety in the field of pharmaceutical sciences. Several prominent anti-cancer medicines reportedly include a pyridine component (33). In addition, an essential function of pyridine in medicinal chemistry is to increase water solubility due to its low basicity and catalytic property (34, 35). This study aims to investigate the mechanism of the RT derivative DH_22, in inducing apoptosis focused on discovering the mechanism of c-Myc in order to provide patients with a reference for selecting a more appropriate therapy.

1.2 Objective

1.2.1 To investigate the anti-cancer effect of renieramycin T derivative DH_22 on lung cancer cells.

1.2.2 To evaluate the mechanism of renieramycin T derivative DH_22 underlying the regulation of c-Myc pathway.

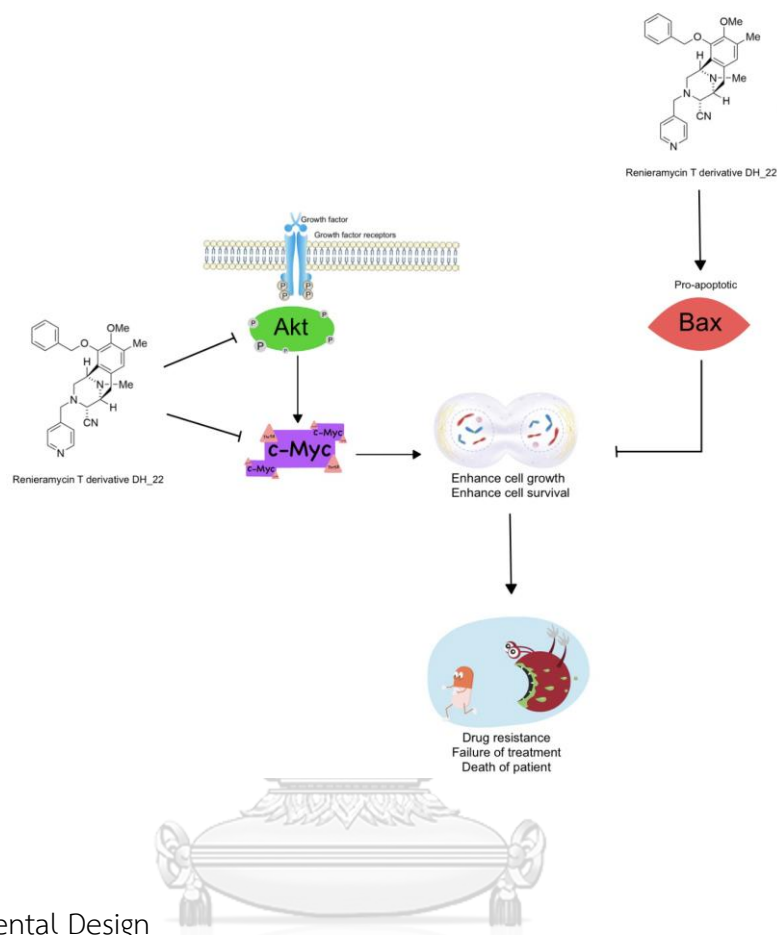
1.3 Hypothesis

Renieramycin T derivative DH_22 has the ability to trigger the death of lung cancer cells via the apoptosis mechanism by inhibiting the production of c-Myc protein.

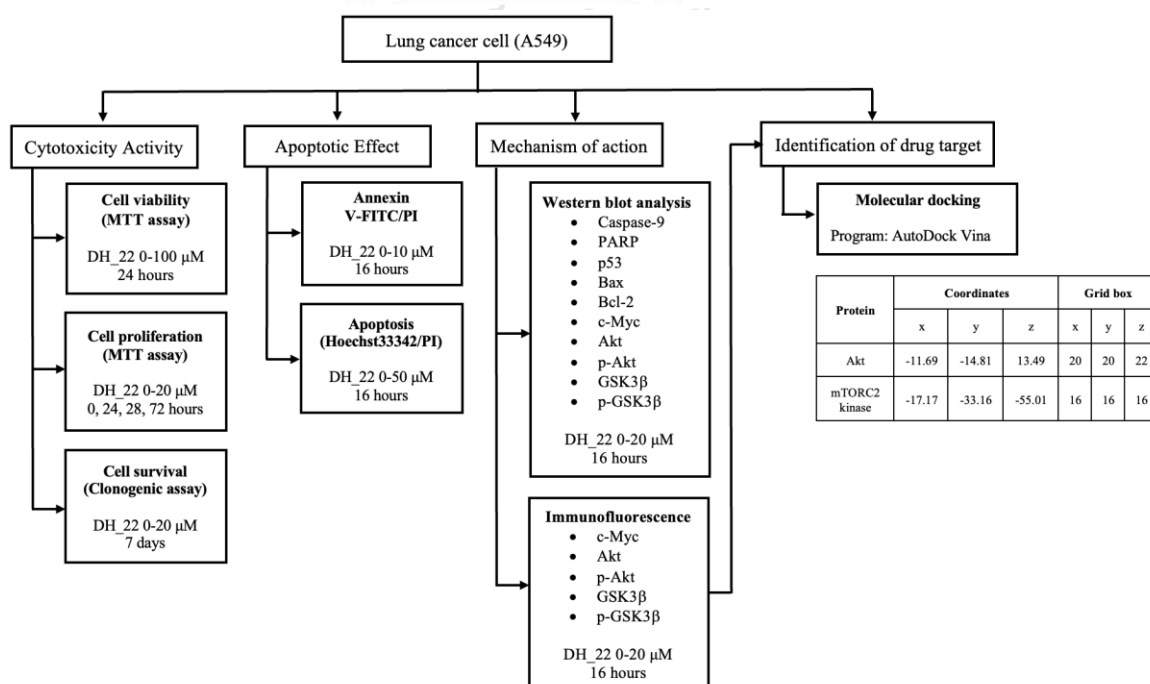
1.4 Expected Benefit

The information about Renieramycin T derivative DH_22 that has the ability to trigger the death of lung cancer cells via the apoptosis mechanism by inhibiting the production of c-Myc protein.

1.5 Conceptual Framework



1.6 Experimental Design



CHAPTER II

LITERATURE REVIEW

2.1 Lung Cancer

Lung cancer is the leading cause of cancer-related death worldwide, accounting for an estimated 1.8 million deaths and more than 2 million new cases each year. In 2020, it was estimated that there will be around 9.5 million cancer-related deaths across all ages and sexes (Figure 1) (1). Approximately one-fifth of these fatalities were attributable to lung cancer. Lung cancer is most prevalent in adults aged 45 to 75. In societies with a lengthy history of tobacco use, 80-90% percent of illnesses are attributable to cigarette smoking (36).

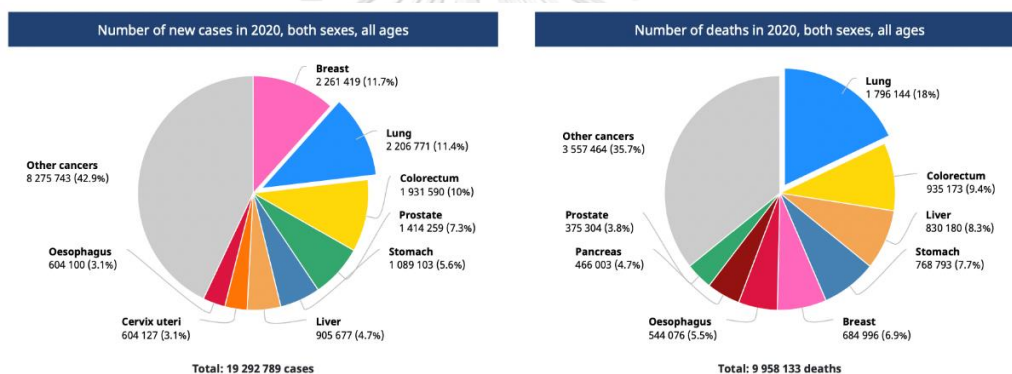


Figure 1. Percentage of new cases and deaths from cancer worldwide in 2020 by different cancer types.

Tumours can develop in any part of the lung, but symptoms may not appear until the disease has progressed or moved to another part of the body. Shortness of breath, chest pain, bloody sputum, unexplained weight loss, persistent coughing or wheezing, and susceptibility to lower respiratory infections are the most prevalent symptoms. Visible tumors, jaundice, and bone pains may arise when cancer spreads beyond the lungs (37, 38). The incidence of lung cancer varies by more than 20-fold between locations, with the highest incidence happening in developing countries with the greatest prevalence of cigarette smoking. Lung cancer is the most frequent cancer in 37 nations, including Russia,

Canada, the United States, China, Southeast Asia, and parts of Eastern Europe (Figure 2) (39).

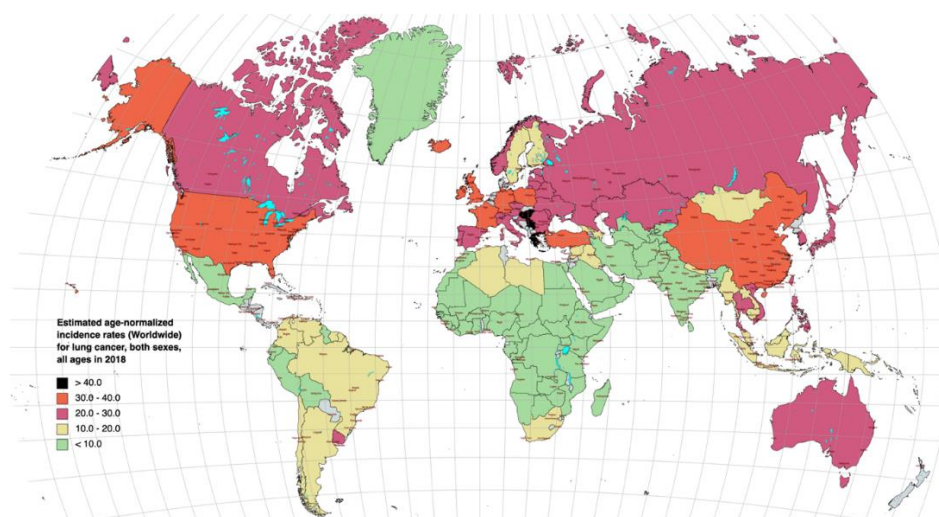


Figure 2. Map showing estimated age-adjusted incidence rates for lung cancer globally in 2020 for both sexes and all ages.

Risk factors of lung cancer

However, lung cancer risk is increased by a number of other variables. Tobacco smoking is the most significant and pervasive lung cancer risk factor. Tobacco smoke contains over 7,000 chemicals, including at least 69 known carcinogens and other toxins linked to severe diseases. Secondhand smoke, also known as side-stream smoke, is an indirect exposure to carcinogens caused by the use of tobacco products. It has been discovered that the urine of nonsmokers exposed to cigarette smoke contains nicotine, its metabolite cotinine, and DNA adducts from tobacco carcinogens. In addition, radon exposure has been related to an elevated risk of lung cancer. Radon is generally found in basements, cellars, and dwellings on the ground floor. As uranium and thorium decay, radioactive radon is released from the soil (40).

Since the advent of genome-wide association (GWA) research approximately 17 years ago, scientists have been more carefully analyzing the human genome in search of correlations between inherited single nucleotide polymorphisms (SNPs) and human disease. GWA studies have successfully

discovered genetic variables that are significantly linked with lung cancer susceptibility, and particular loci have been narrowed to subgroups such as gender, ethnicity, smoking status, and histological subtypes (41). Furthermore, a family history of lung cancer, certain vitamins, and radon and asbestos exposure are also risk factors for lung cancer (42).

Type of lung cancer

Cancer is linked to the patient's smoking behaviour. Lung cancer is classified into two types: small cell lung cancer (approximately 15% of all instances) and non-small cell lung cancer (NSCLC), which accounts for roughly 85% of all cases. Adenocarcinoma, squamous cell carcinoma, and giant cell carcinoma are the three types of NSCLC. However, SCLC is malignant and more aggressive than NSCLC (43). Squamous cell carcinoma is cancer that accounts for 30% of all NSCLC. This cancer is usually seen in the center of the chest with slow growth. The period from tumor growth to symptoms in years.

Adenocarcinoma lung cancer is cancer that occurs in female patients or non-smokers. This cancer is the most common and has a higher tendency to metastasize than other lung cancers. This cancer usually grows at a rate similar to squamous cell carcinoma. This cancerous growth tends to grow towards the periphery of the lung. Large cell cancer is the least common form of cancer. Cancer metastasizes faster than squamous cell carcinoma. These tumors grow in the area of the peripheral location. Small cell cancer accounts for about 15% of total lung cancer cases. In general, patients with this type of lung cancer have the same metastatic time as the time of diagnosis (44).

Treatments

The patient's overall health, the stage or severity of the illness, and the kind of cancer all have a role in selecting the course of therapy. Stage I cancer is restricted to the lungs, stage II cancer to the lungs and ipsilateral hilar, peribronchial, and bronchopulmonary nodes, stage IIIB cancer to contralateral mediastinal or supraclavicular nodes, and stage IV cancer to distant dissemination

(45). Genetic testing results, which can detect changes that make some lung cancers receptive to specific drugs, may also influence the type of treatment a patient receives. Tumor removal is typically performed surgically in patients with stage I, II, and III NSCLC in cases where the tumor may be surgically removed without causing irreversible damage to the patient. Surgeons can take off the section or lobe of the lung that contains the tumor (46).

Some individuals who have resection of lung cancer may benefit from adjuvant treatment. Radiation treatment, chemotherapy, and targeted therapy are all examples of adjuvants. Patients with NSCLC who are in stages IIA, IIB, or IIIA get chemotherapy following surgery to eradicate cancer cells and extend their chances of life (47). Approximately 40% of persons with newly diagnosed lung cancer cases are already in stage IV. The treatment goals for these individuals are to improve patients' chances of surviving the condition and lessen the severity of disease-related consequences. First-line therapy for patients with stage IV non-small cell lung cancer is cytotoxic combination chemotherapy. Histology, age versus comorbidities, and the patient's performance level are all factors that may lead to a modification of this treatment (48).

Radiotherapy is a form of palliative care that can be used on patients with NSCLC whose cancer has not responded to surgery or chemotherapy to increase their comfort level (49, 50). With high-powered lasers, radiotherapy can destroy cancer cells by destroying their DNA. Cancer in particular body parts may be reduced or eliminated using this treatment. Patients with localized thoracic NSCLC who are not surgical resection candidates may benefit from radiation therapy.

2.2 Apoptosis

The process of programmed cell death must have apoptosis as one of its components to be effective. It can occur not only due to the loss of cells or the stress caused by the environment but also during normal growth and morphogenesis. Many different types of the executioner and regulatory molecules work together to keep apoptosis under strict control. Apoptotic cell death is characterized by chromatin condensation, membrane blebbing, DNA breakage,

nuclear shrinkage, and a lack of adherence to the extracellular matrix. In addition, the cell's metabolism shifts, releasing phosphatidylserine into the surrounding environment and activating caspases, which kill the cell (51).

There are two primary ways in which apoptosis can be triggered: the extrinsic pathway and the intrinsic pathway. The mitochondria are responsible for the intrinsic process. In contrast, the death receptor controls the extrinsic pathway, which involves the transmission of death signals, eventually result in the same final result (execution pathway) (52). When extracellular ligands such as tumor necrosis factor (TNF), fas ligand (Fas-L), and tumor necrosis factor-related apoptosis-inducing ligand (TRAIL) bind to the extracellular domain of the death receptor (transmembrane receptors), such as the type 1 TNF receptor (TNFR1), Fas, and TRAIL receptors, the extrinsic pathway is triggered. This pathway is also known as the death receptor pathway. Caspases appear to play an excessive part in the process of apoptosis, as indicated by experimental findings. Caspases are essential for initiating and executing apoptosis, and their specific substrate preferences are determined by their three-dimensional structures.

Caspases with large pro-domains interact with other proteins and signaling pathways. The death effector domain (DED) and the caspase recruitment domain are two of these pro-domains (CARD). DED contains Caspase-8 and Caspase-10, whereas CARD has Caspase-1, Caspase-2, Caspase-4, Caspase-5, Caspase-9, Caspase-11, and Caspase-12. Caspases are classified into two categories in apoptotic signaling cascades: initiators and effectors (53).

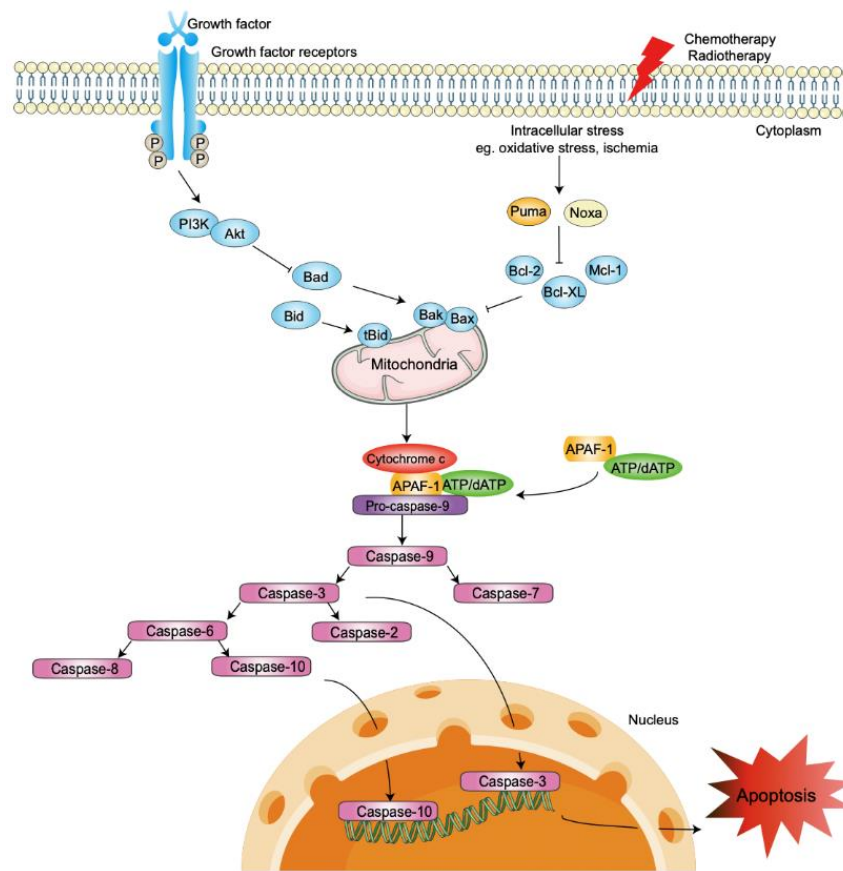


Figure 3. Intrinsic apoptosis pathway, internal cellular stress initiates the intrinsic pathway of apoptosis, also known as the mitochondrial pathway.

On the other hand, mitochondrial-mediated apoptosis occurs through the intrinsic route (Figure 3) (54). Radiation, oxidative stress, and cytotoxic drugs can all activate the intrinsic pathway. The insertion of Bax/Bak into the mitochondrial membrane and the subsequent release of cytochrome c into the cytoplasm make up the intrinsic route. The proteins Bcl-2 and Bcl-xL prevent cytochrome c from being released.

An apoptosome is a multiprotein complex that triggers caspase 9 and caspase 3 to activate the caspase cascade, ultimately resulting in cell death and apoptosis. The apoptosome comprises cytochrome c, apoptosis-associated factor 1, and procaspase-9. Several proteins are involved in the intrinsic pathway, including SMAC/DIABLO, Caspase-9, Bcl-2, Bcl-w, Nox, Aven, and Myc (oncogene Myc).

Mitochondrial dysfunction causes loss of inner mitochondrial membrane potential, increased superoxide ion production, disruption of mitochondrial biogenesis, efflux of matrix calcium glutathione, and membrane protein release; these effects have therapeutic potential in cancer treatment by inducing apoptosis in cancer cells (53, 55).

2.2.1 p-Akt

Protein kinase B (PKB), commonly known as Akt, is an oncogenic protein that affects cell survival, proliferation, growth, apoptosis, and glycogen consumption (56). Akt phosphorylates proteins such as GSK3, Bcl-2-associated death promoter, forehead in rhabdomyosarcoma, and mouse double minute 2 homolog after being triggered by phosphorylation at Thr308 or Ser473 (57). Because of the signals it creates that disturb the normal regulatory mechanisms activating mTOR, phosphorylated Akt (p-Akt) has been related to the abnormal regulation of apoptosis, cell proliferation, and cell motility (58, 59).

Two Akt phosphorylation sites (T308 and S473) are essential for regulating various physiological processes (60). High p-Akt expression is significantly related to a negative prognosis for NSCLC patients (61). In response to nutrient deprivation, 13 of 19 lung cancer cell lines showed constitutive p-Akt (Ser473) expression (62). The percentage of Akt-positive samples in cancer and surrounding tissues was 76.45% (39/51) and 38.46% (5/13), respectively, in a study of lung cancer tissues (63). It has been hypothesized that improved upstream signaling is responsible for the activation.

p-Akt expression has previously been linked to poor differentiation and lymph node metastasis in NSCLC, and Akt activation is assumed to be critical in lung cancer development. p-Akt was discovered in significant quantities in NSCLC tissues and premalignant bronchial epithelial tissues but not in normal cells, showing that Akt activation is implicated in the precancerous lesion process that leads to the formation of NSCLC in bronchial epithelial cells (19). To conclude, greater p-Akt expression and the oxidative stress response in

which it is involved may be linked to a worse overall survival rate in cancer patients. Patients with haematological malignancies with p-Akt overexpression, in particular, may have a poor prognosis due to their condition. Furthermore, there is evidence that p-Akt may one day be used as a therapeutic target in cancer therapy (64).

2.2.2 c-Myc

c-Myc, a proto-oncogene transcription factor, affects multiple downstream signaling pathways. c-Myc is involved in the formation of the cell cycle, cell survival metabolism, and stem cell activities (Figure 4) (65) (66). Overexpression of the c-Myc protein leads to the aggressiveness and treatment resistance of cancers. This is due to the fact that overexpression of the protein causes stemness characteristics to be overactivated (22). Akt regulates the protein's stability, which determines whether or not c-Myc is present in cells. Akt inhibits c-Myc breakdown by preventing phosphorylation at the protein degradation site, threonine 58 (Thr58) (67).

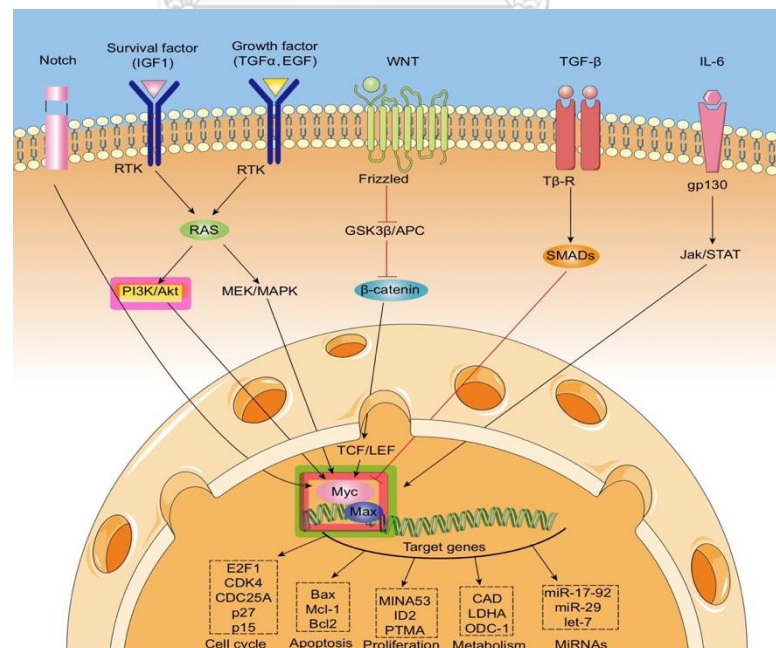


Figure 4. c-Myc signaling pathway, overexpression of c-Myc causes carcinogenesis, and it can be a potential target for anti-cancer treatment.

c-Myc is a transcription factor expressed constitutively and abnormally in approximately 70% of human malignancies (68). Previous studies have shown that inhibiting Myc's activity can lead to tumors' regression by either re-establishing normal cell checkpoint processes or inducing proliferative arrest, cellular senescence, and apoptotic mechanisms (69). One of the most effective processes for controlling the amount of Myc protein in the cell is called the ubiquitin-proteasome system, which degrades proteins. The first phase in this process involves the attachment of ubiquitin molecules to the proteins that are being degraded, and the second step involves the degradation of poly-ubiquitinated proteins by 26S proteasomes that contain at least four ubiquitin molecules each (70).

In the therapy of cancer, several various approaches can be taken to target myc. These include lowering the expression of myc protein, preventing the dimerization between myc and max, and triggering myc destruction by the ubiquitin-proteasome system (8). Several investigations have indicated that c-Myc interacts with other self-renewal transcription factors including as Sox2, Nanog, and Oct4. These three self-renewal transcription factors play an important role in stemness. In conjunction with other factors, c-Myc stimulates cell self-renewal. The current study found that c-Myc affects other self-renewal transcription factors via boosting protein transcription and activity (22). As a result, blocking Akt, upstream of many regulators relevant to cancer, can be a useful therapeutic strategy.

2.3 Renieramycin T derivative DH_22

Renieramycin T (RT) is a tetrahydroisoquinoline alkaloid molecule from the renieramycin family identified from the blue sponge *Xestospongia* sp. in 2009 by pre-treatment with potassium cyanide [45]. Renieramycin T derivative DH_22 was synthesized from renieramycin T (RT) and obtained the compound from the laboratory of Prof. Masashi Yokoya, Meiji University, Japan.

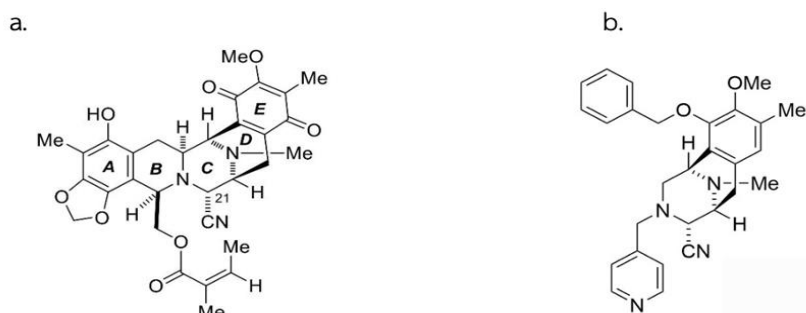


Figure 5. Structure of renieramycin T (RT) and renieramycin T derivative DH_22.

Anti-cancer properties of renieramycin T have recently been revealed in non-small cell lung (H292, H460, and QG56) (30), breast (T47D), colon (HCT116), prostate (DU145) (29), and pancreatic (AsPC1) cancer cells (28). Nanomolar concentrations of amino nitriles were discovered to promote the cytotoxic activity of compounds consisting of the right-half moiety of renieramycin (CDE-ring) (71). Renieramycin T DH_22 preserves the CDE-ring. Consequently, DH22 will enhance cytotoxicity and an intriguing chemical. Furthermore, earlier research demonstrated that the effects of RT on the apoptotic pathway are dependent on the disappearance of Mcl-1 via an increase in Mcl-1 protein degradation.

CHAPTER III

METHODOLOGY

3.1 Preparation of DH₂₂ Stock Solution

The solid compounds were dissolved in DMSO to prepare a 50 mM stock solution and kept at 20 °C. It was newly diluted to the concentrations required in the research, with the assumption that the final DMSO concentration should be less than 0.05%.

3.2 Cell Lines and Culture

A549 (ATCC® CCL-185TM, RRID: CVCL 0014) human non-small cell lung cancer (NSCLC) cell lines were used because it derived from human lung carcinoma and exhibit characteristics similar to lung adenocarcinoma, which is one of the most common types of lung cancer. The A549 cells were obtained from the American Type Culture Collection (Manassas, VA, USA). Dulbecco's Modified Eagle Medium (DMEM) was used to culture the A549 cells. The medium was maintained at 37°C with 5% CO₂ in a humidified incubator, it contained 10% FBS, 2 mM L-glutamine, and 100 units/mL of penicillin and streptomycin.

3.3 Cytotoxicity Assay

The A549 lung cancer cells (1×10^4 cells/well) were seeded in a 96-well plate and incubated overnight. The next day, the cells were treated with 0 – 100 μ M of renieramycin T derivative DH₂₂ for 24 hours at 37°C, followed by the 3-(4,5- dimethylthiazol- 2- yl) - 2,5- diphenyltetrazolium bromide (MTT) solution (Sigma Chemical, St. Louis, MO, USA). 100 μ L (4 mg/mL in PBS) was added to each well. The plate was kept in the incubator for four hours at 37°C.

After that, the MTT reagent was discarded, and 100 μ L of dimethyl sulphoxide (DMSO) was added to solubilize the formazan crystals. A microplate reader (Anthros, Durham, NC, USA) was used to measure the formazan product

at 570 nm. The half maximal inhibitory concentration (IC_{50}) in different groups was calculated by GraphPad Prism 9 software (GraphPad Software Inc., San Diego, CA).

$$\text{Percentage of cell viability} = \frac{\text{Absorbance of treated cells}}{\text{Absorbance of control cells}} \times 100$$

3.4 Annexin V-FITC/PI Staining Apoptotic Assay

A549 cells were seeded (5×10^4 cells/well) and treated for 16 h with varying concentrations of DH-22 (0-10 μM). Then, cells were centrifuged, washed twice with PBS, and suspended in binding buffer. The cells were then stained for 15 min at room temperature with 2.5 μl of Annexin V-FITC and 1 μl of PI according to the manufacturer's protocol (ImmunoTools, Friesoythe, Germany). The Guava easyCyte flow cytometer was used to examine live, apoptotic, and necrotic cells (EMD Millipore, Hayward, CA, USA).

3.5 Nuclear Staining Assay (Hoechst33342/PI)

Hoechst 33342 and PI double staining methods were used in the nuclear co-staining to differentiate between apoptotic and necrotic cell death. In a 96-well plate, A549 cells were seeded at a density of 1×10^4 cells/well. The plate was incubated overnight to allow for the cells to adhere. After that, it was treated with 0–50 μM concentration of renieramycin T derivative (DH_22) and incubated for 24 hours. Then, the cells were stained with 10 $\mu\text{g/mL}$ of Hoechst 33342 (Sigma, St. Louis, MO, USA) and 0.02 $\mu\text{g/mL}$ propidium iodide (PI) (Sigma, St. Louis, MO, USA) for 30 minutes. The fluorescent microscope was used to visualize the cell. The percentage of apoptotic cells was calculated by counting the number of condensed nuclear and DNA-fragmented cells.

$$\text{Percentage of apoptotic cells} = \frac{\text{Number of apoptotic cells}}{\text{Total of apoptotic and non-apoptotic cells}} \times 100$$

3.6 Western Blot Analysis

The Western blot method was used to measure the quantity of specific proteins in cells. A549 cells were seeded in six-well plates at a density of 4×10^5 cells/well overnight. Renieramycin T derivative, DH_22, was then applied to the cells for 16 hours with a concentration of 0-20 μM . After being washed with ice-cold 1X PBS, the cells were scratched in RIPA buffer containing 1% Triton X-100, 100 mM PMSF, and a protease inhibitor cocktail on ice tablets for 40 minutes, followed by 15 minutes of centrifugation at $12,000 \times g$ and 4°C . The protein concentrations were determined using a BCA protein assay kit by Pierce Biotechnology (Rockford, IL, USA).

Samples were denatured by heating at 95°C for five minutes in a loading buffer and then were loaded into 10% sodium dodecyl sulfate-polyacrylamide gel electrophoresis (SDS-PAGE). After that, it was transferred to 0.2 μm polyvinylidene difluoride (PVDF) membranes (Bio-Rad Laboratories, Hercules, CA, USA). 5% Non-fat dry milk in TBST (25 mM Tris-HCl, pH 7.4, 125 mM NaCl, and 0.05% Tween 20) was used to block the transferred membranes for 1 hour at room temperature.

The next step was the incubation overnight at 4°C with the specific primary antibodies. After three washes with TBST, the membranes were incubated with horseradish peroxidase-coupled isotype-specific secondary antibodies anti-rabbit or anti-mouse (1:2000 in 5% w/v skim milk in TBST) at room temperature for one hour. A chemiluminescence substrate was used to observe the complex's reactive properties, and then an X-ray film was used to record the results. The ImageJ program was used to assess protein band intensity (version 1.52, National Institutes of Health, Bethesda, MD, USA).

3.7 Proliferation Assay

In a 96-well plate, A549 lung cancer cells (2×10^3 cells/well) were seeded and incubated overnight. The cells were then treated the following day with 0-20 μM renieramycin T derivative DH_22 for 0, 24, 48, and 72 hours at 37°C ,

followed by 3-(4,5-dimethylthiazol-2-yl)-2,5-diphenyltetrazolium bromide (MTT) solution (Sigma Chemical, St. Louis, MO, USA). 100 μL (4 mg/mL in PBS) was added to each well. The plate was incubated at 37°C for 4 hours. The MTT reagent was then removed, and 100 μL of dimethyl sulfoxide (DMSO) was added to dissolve the formazan crystals. The formazan product was measured at 570 nm using a microplate reader (Anthros, Durham, NC, USA).

3.8 Clonogenic Cell Survival Assay

The clonogenic assay is commonly used for assessing individual cells' ability to proliferate and form colonies. A549 cells were seeded (250 cells/well) in six-well plate and incubated overnight. The next day, the cells were treated with 0-20 μM of renieramycin T derivative DH_22 and incubated for an additional 7 days. After seven days incubation, the cells were fixed and stained with the DNA intercalating dye, 0.1% crystal violet for 30 minutes, then washed with PBS several times. The results were manually quantified using ImageJ.

3.9 Immunofluorescence

Immunofluorescence uses the specificity of antibodies with fluorescent dyes or fluorophores to detect their antigen. A549 cells were seeded at a density of 1×10^4 cells/well in 96-well plates and incubated overnight. After 16 hours of renieramycin T derivative (DH_22) treatment in 0-20 μM concentrations, the cells were first fixed in 4% paraformaldehyde for 15 minutes. This was followed by permeabilization in 0.5% Triton-X for five minutes, then blocking with 10% FBS in 0.1% Triton-X in PBS for one hour at room temperature. Following this, the cells were probed at 4°C overnight with primary antibodies.

Next, an alexa fluor 488 IgG anti-rabbit secondary antibody (Invitrogen) was added and incubated for one hour at room temperature. The cells were then co-stained for 15 minutes with 10 $\mu\text{g/mL}$ Hoechst 33342. PBS was used to wash the cells, and 50% glycerol was used to fix them. The photos were examined

using a fluorescence microscope, and the fluorescence intensity was calculated using ImageJ software. (Image J 1.52a, Rasband, W., National Institutes of Health, USA).

3.10 Molecular Docking

The technique of molecular docking was utilized in order to identify any potential interactions between DH-22((5S,7S,8R,9S)-4-(benzyloxy)-3-methoxy-2,11-dimethyl-7-(pyridin-4-ylmethyl)-5,6,7,8,9,10-hexahydro-5,9-epiminobenzo[8]annulene-8-carbonitrile) and the Akt protein (PDB ID 6S9W). The chemical structure of the ligand then was constructed with the help of the software Gaussian09 in order to be ready for the docking investigation.

After that, the geometry of each chemical was optimized by using ab initio calculation with Hartree-Fock method 6-31G basis set. The pdbqt file of the protein and ligand was prepared using AutoDock tools 1.5.6. AutoDock Vina is utilized to complete the docking analysis computations. The ligand is then docked into the location of Akt's native ligand binding site. The grid was centered at the position at the x, y, and z coordinates of -11.69, -14.81, and 13.49 respectively. The grid box size is adjusted to have dimensions of 20 by 20 by 22 angstroms. The graphical representation of the data was accomplished with the help of the Discovery Studio Visualizer by BIOVIA.

3.11 Statistical Analysis

The results were provided as means \pm SEM of at least three biological replicated samples. Statistical differences were analyzed by Graph Pad Prism 9 software (GraphPad Software Inc., San Diego, CA) using a post hoc Turkey test. Statistical significance is determined at $p < 0.05$.

CHAPTER IV

RESULTS

4.1 Cytotoxicity and Apoptosis-Inducing Effect of Renieramycin T Derivative DH_22

The right-half structure of renieramycin T, which was discovered in the Thai blue sponge *Xestopongia* sp., served as the starting material for the synthesis of DH-22. The step-by-step synthesis of DH_22 is shown in Figure 6. The synthesis was done in the laboratory of Professor Yokoya, Meiji University.

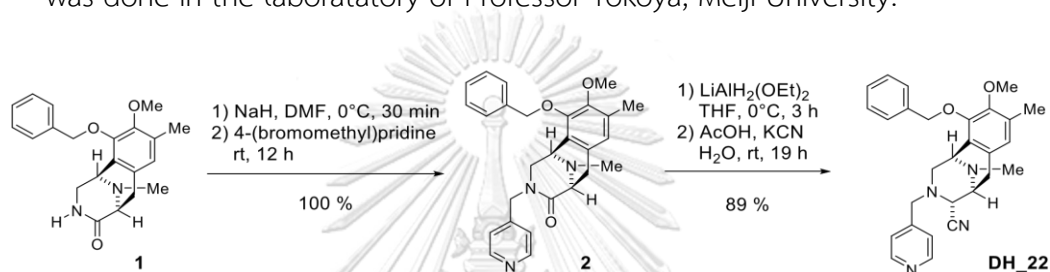


Figure 6. Synthesis of the renieramycin T derivative DH-22.

This study examined the cytotoxic profile of DH-22 in non-small cell lung cancer (NSCLC) A549 cells to discover its possible anti-cancer effects. The cells were incubated with DH-22 (0–100 μM) for 24 h. The findings show that DH-22 decreased the viability of A549 cells considerably (Figure 7A), with half maximum inhibitory concentration (IC₅₀) of DH-22 of $13.27 \pm 0.66 \mu\text{M}$. Flow cytometric analysis of apoptosis and necrosis using annexin V-FITC/PI staining was conducted to confirm the type of cell death (Figure 7B and C). A549 cells were treated for 16 h with DH-22 (0–10 μM), and the findings revealed that the cytotoxic effect is due to apoptotic cell death.

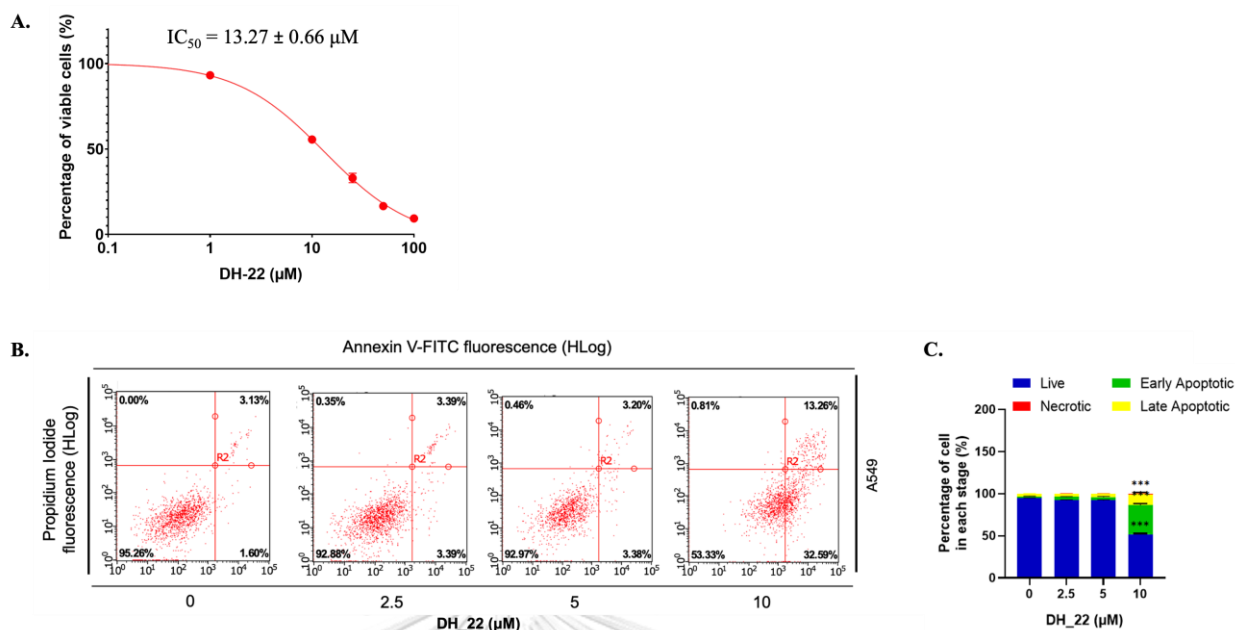


Figure 7. Effect of DH-22 on cell viability and apoptotic cell death in the NSCLC cell line A549.

(A) A significant decrease in cell viability after 24 h exposure to DH-22 is observed with the half maximum inhibitory concentration (IC_{50}) of $13.27 \pm 0.66 \mu\text{M}$. (B) After 16 h of treatment with DH22, apoptotic and necrotic A549 cells were determined using Annexin V-FITC/PI staining and flow cytometry. (C) Percentage of each cell death-type as determined using flow cytometry. All data are presented as means \pm SEM ($n = 3$). *** $p < 0.001$ compared with untreated cells.

4.2 DH-22 therapy demonstrates apoptotic characteristics

Morphological characteristics have been accepted as accurate indicators of apoptosis. Microscopy demonstrates nuclear condensation, cell contraction, and cell fragmentation into apoptotic bodies. The nuclear morphology of DH-22-treated cells was analyzed using Hoechst 33342. A549 cells were treated with 0–50 μM DH-22 for 16 h. Propidium iodide (PI) was also utilized to identify necrotic cell death. Exposure to DH-22 (0–50 μM) resulted in apoptotic cell death, which was clearly indicated by the detection of DNA condensation and/or fragmentation (Figure 8A and B). Similarly, treatment with the increasing

concentrations of DH-22 resulted in decreased cell viability and increased percentage of apoptotic cells.

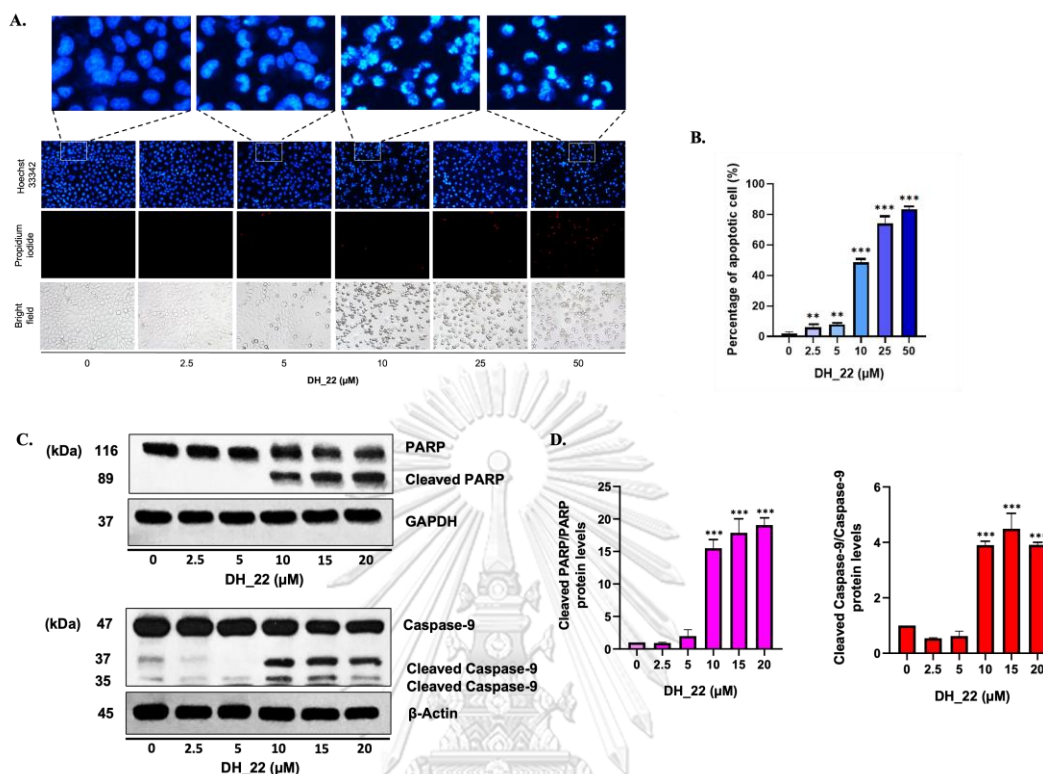


Figure 8. Apoptotic characteristics of renieramycin T derivative DH_22 treatment. (A) After A549 cells were treated with DH-22 for 16 h Hoechst 33342/PI staining was used to stain the cell nuclei. (B) The percentage of apoptotic cells as determined by Hoechst/PI staining. (C) Treatment with-20 μM DH-22 for 16 h induces cleavage of PARP and Caspase-9. (D) The average relative density. The data is presented as mean ± SEM (n = 3). * $p < 0.05$, *** $p < 0.001$ compared to untreated control cells.

Furthermore, a novel approach to studying the presence of apoptosis is to demonstrate the activation of downstream caspases. This can be achieved using western blotting of target proteins cleaved by caspases, or DNA repair enzymes. Increased levels of the apoptotic marker proteins cleaved caspase-9 and cleaved poly (ADP-ribose) polymerase (PARP) were found in treated cells (Figure 8C and D). Caspase-9 is an initiator caspase that is activated by the intrinsic apoptotic pathway and cleaves effector caspases, ultimately resulting in apoptosis. During

apoptosis, PARP is cleaved by caspases, resulting in the loss of its enzymatic activity and the accumulation of PARP fragments.

4.3 Mechanism of action of DH-22 suppressing lung cancer and inducing apoptosis

The main regulators of p53-dependent apoptosis, such as p53, anti-apoptotic protein (Bcl-2), and pro-apoptotic protein (Bax), were investigated in A549 cells treated with DH-22 (0-20 μM) for 16 h. Bax is a well-known direct target of the p53 tumor suppressor protein. The results demonstrated that p53 and Bax were significantly elevated in response to the DH-22 treatment.

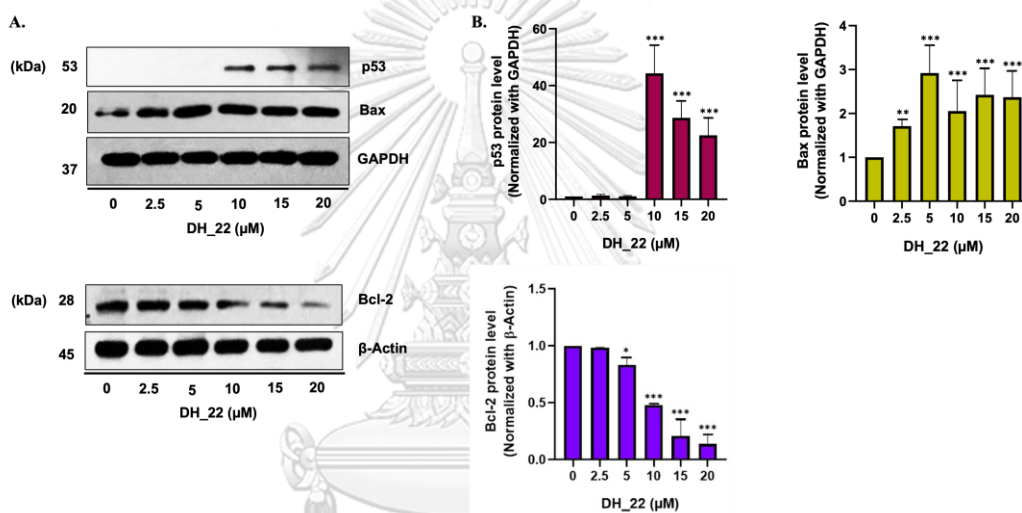


Figure 9. The results of western blot analysis of several proteins.

(A) The levels of apoptosis-associated proteins p53, Bax, and Bcl-2 in A549 cells treated with DH-22 (0-20 μM) for 16 h. (B) The average relative density. The data is presented as mean \pm SEM (n = 3). * p <0.05, *** p <0.001 compared to untreated control cells.

However, the levels of the anti-apoptotic protein Bcl-2 were reduced (Figure 9). The reduction of Bcl-2 is a crucial step in the early stages of apoptosis. It permits caspases and other pro-apoptotic factors to be activated, resulting in cell death. These findings demonstrate that DH-22 induces apoptosis in A549 cells *via* stimulating p53-dependent pathways and altering critical regulatory proteins.

4.4 Cell proliferation and survival effect of renieramycin T derivative DH_22

The MTT (3-(4,5-dimethylthiazol-2-yl)-2,5-diphenyltetrazolium bromide) proliferation test measured cell viability and metabolic activity. A549 cells were treated with the RT derivative DH_22 (0-20 μM) and incubated for various periods of time (0, 24, 48, and 72 hours). The findings showed that the compound is extremely efficient in killing cancer cells. Furthermore, the clonogenic assay was used to assess the compound's growth-inhibitory effects on cancer cells (Figure 10).

The findings showed that DH_22 efficiently suppressed cancer cell proliferation, as evidenced by the following observations. The cancer cells demonstrated strong colony formation in the absence of the compound, suggesting their capacity to proliferate and form colonies. In contrast to the control group, cells treated with DH_22 demonstrated a significant reduction in colony formation. This showed that the compound has a strong inhibitory effect on cancer cells' ability to grow and form colonies.

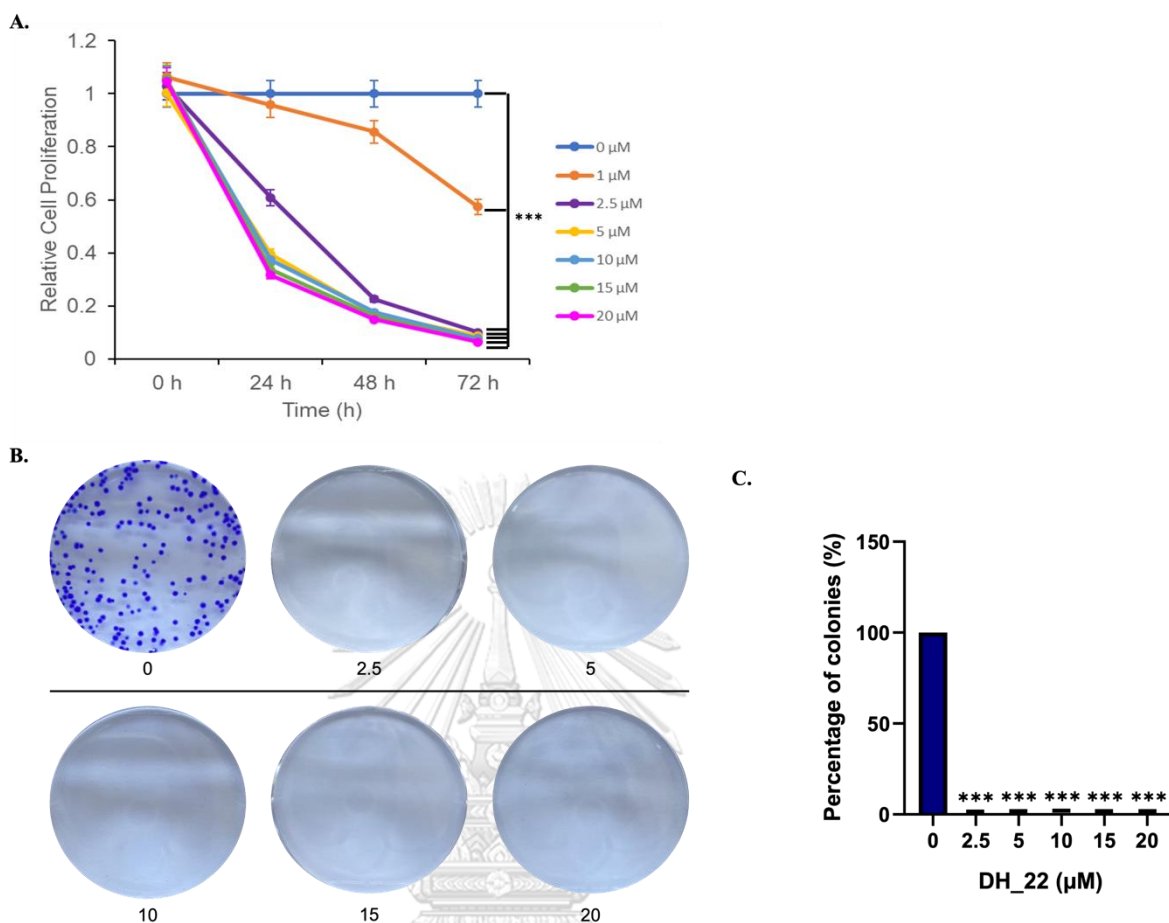


Figure 10. DH₂₂ has a strong inhibitory effect on A549 cells.

(A) Cell proliferation profiles in various intervals demonstrated DH₂₂'s potential to eliminate cancer cells. (B) DH₂₂ significantly reduced colony formation in A549 cells as compared to control. (C) The results showed that DH₂₂ suppressed single colony development at all doses. All data are presented as means \pm SEM ($n = 3$). *** $p < 0.001$ compared with untreated cells.

4.5 Inhibition of survival regulators by renieramycin T derivative DH₂₂ therapy

Further investigations are warranted to elucidate the underlying mechanisms of action and to investigate its therapeutic potential in the context of cancer treatment. The signaling molecules involved in cell survival and proliferation are the primary regulators of apoptosis. These include Akt and c-Myc, as they are crucial components of cell survival, cell proliferation, and cell stemness for the progression of cancer. We used western blot analysis and

immunofluorescence labeling to demonstrate how DH_22 inhibits the Akt/c-Myc signaling pathway, which subsequently promotes apoptosis.

The A549 cells were treated for 16 hours with 0–20 μM DH_22 before being incubated with primary antibodies against Akt, p-Akt, c-Myc, and GSK3 β . The results showed that the fluorescent intensity of Akt, and p-Akt significantly diminished, where the level of Akt and p-Akt were evenly distributed in both the cytoplasm and nucleus of cells (Figure 11A, D). The immunofluorescence results correlate with the western blot results (Figure 11J, K) indicating the presence of Akt phosphorylation inhibition.

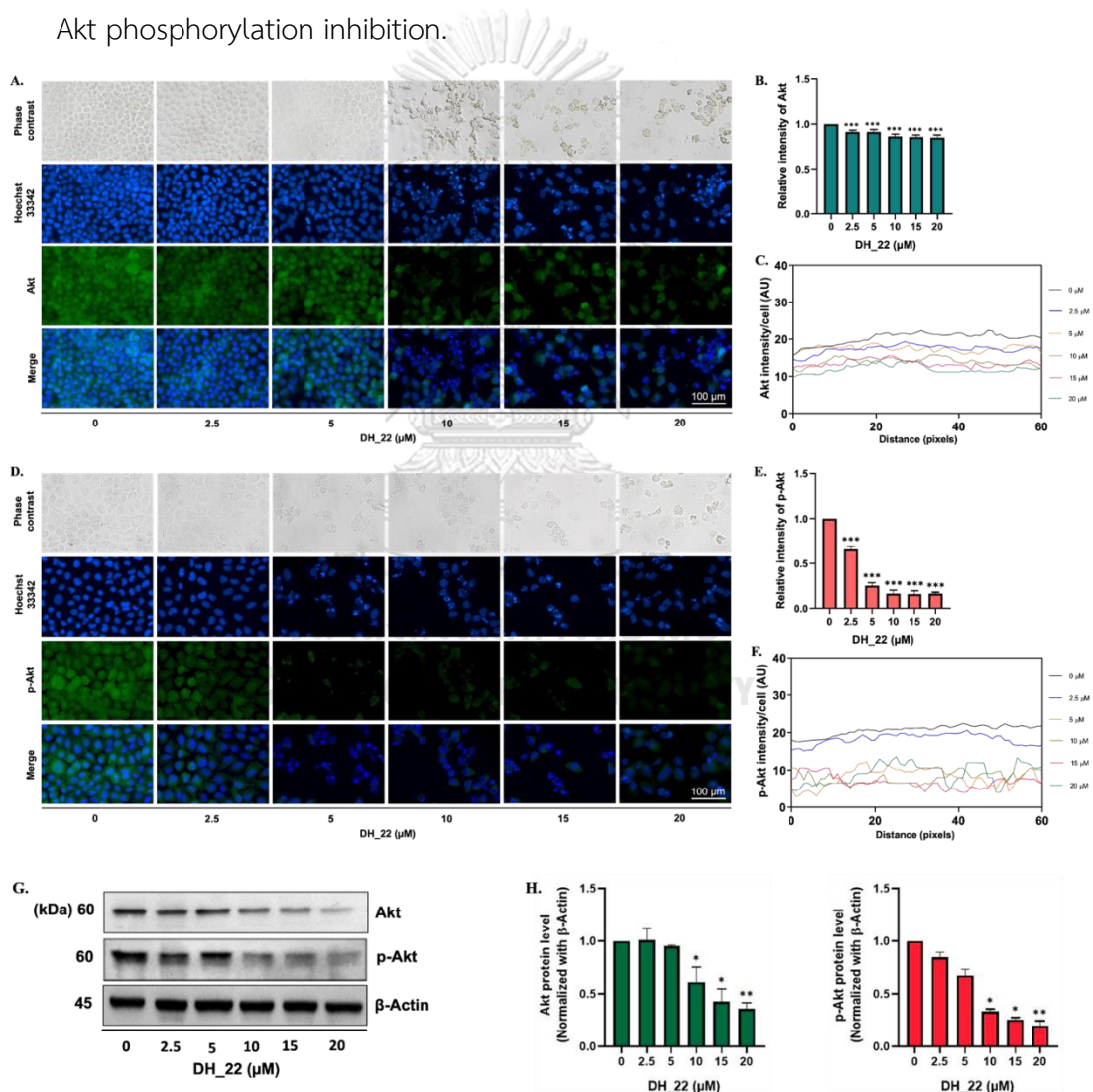


Figure 11. Effect of DH_22 on Akt signaling pathway by immunofluorescence.

(A, D) The cellular levels of Akt and p-Akt of A549 cells treated by DH_22 at 0–20 μM concentrations for 16 hours. (B, E) The relative intensity compared to

untreated control. (C, F) The fluorescence intensity was analyzed by imageJ software. (G) The level of Akt and p-Akt protein expression. (H) Relative protein level. Values are presented as means \pm SEM (n = 3). * p < 0.05 ** p < 0.01, and *** p < 0.001 compared with untreated cells.

The degradation of c-Myc by GSK3 β is critical for regulating its activity and preventing uncontrolled cell proliferation. The increasing results of GSK3 β expression and decreasing of p-GSK3 β in western blot and immunofluorescence experiments were indicating that GSK3 β plays a role in the degradation of c-Myc. This can be proven by the results of c-Myc expression which decreased in intensity on immunofluorescence and western blot band. In addition, c-Myc is predominantly localized within the nucleus in untreated control cell, where it performs its transcriptional regulatory functions. However, if observed in more detail in treated cell of DH_22, c-Myc is detected outside of the nucleus, it might be due to various factors, such as cellular stress, signaling pathways, or specific mutations. GSK3 β plays a negative role (Figure 12) in regulating c-Myc activity by promoting its degradation.

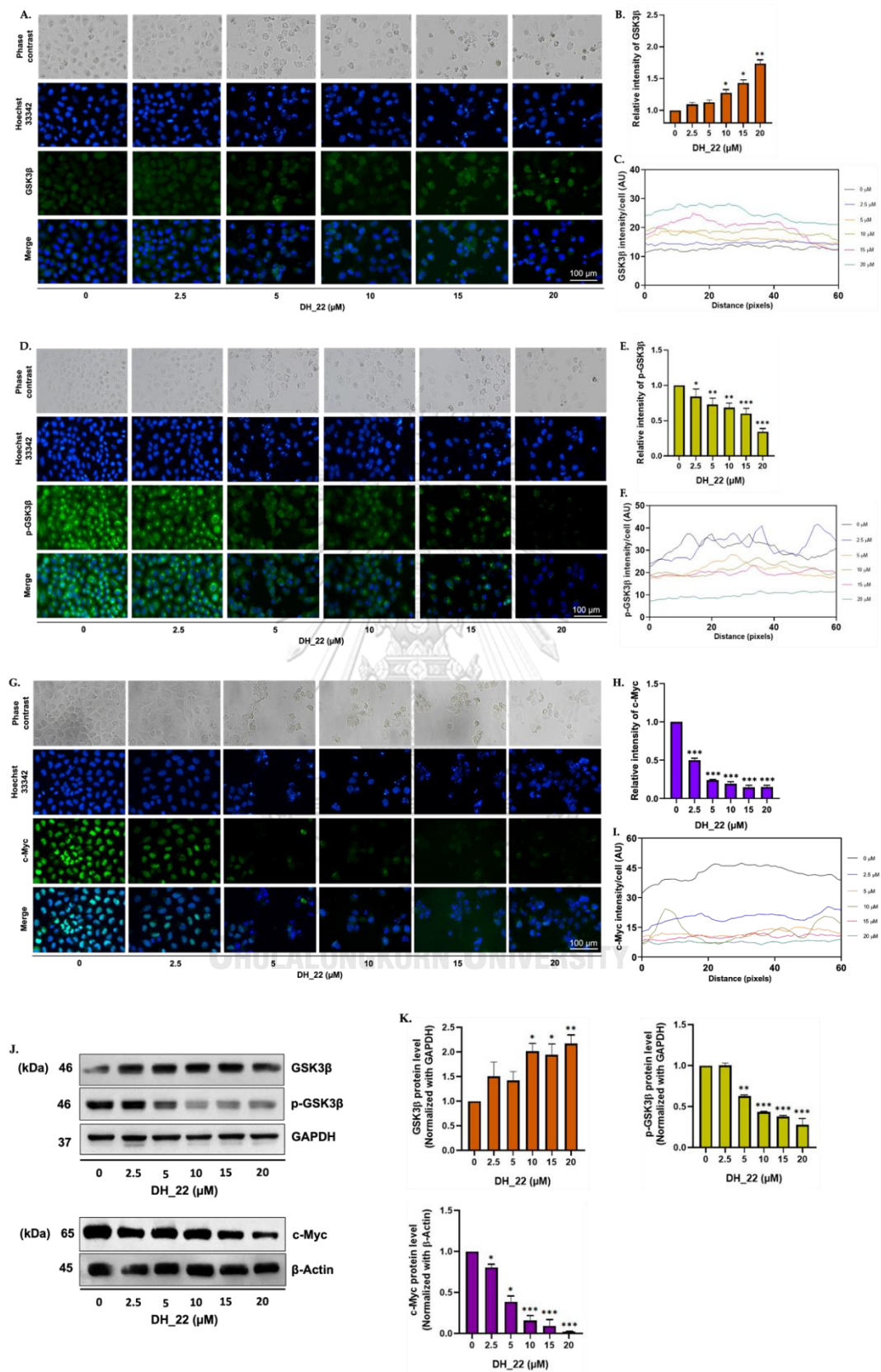


Figure 12. Effect of DH₂₂ on GSK3 β altering c-Myc by immunofluorescence.

(A, D, G) The cellular levels of GSK3- β , and p-GSK3- β , of A549 cells treated by DH_22 at 0–20 μM concentrations for 16 hours. (B, E, H) The relative intensity compared to untreated control. (C, F, I) The fluorescence intensity was analyzed by ImageJ software. (J) The level of GSK3- β , and p-GSK3- β protein expression. (K) Relative protein level. Values are presented as means \pm SEM (n = 3). * p < 0.05 ** p < 0.01, and *** p < 0.001 compared with untreated cells.

4.6 Molecular Docking Simulation Demonstrates the Interaction of DH_22 with the Akt/c-Myc Proteins

To investigate more the mechanism of DH_22 in inducing apoptosis, molecular docking studies were carried out. The target proteins, mTOR and Akt1, were chosen from the immunofluorescence results that DH_22 reduce the expression of p-Akt and c-Myc. The mammalian target of rapamycin (mTOR), especially mTORC2 is one of the key enzymes of Akt phosphorylation, while Akt1 itself plays a significant role in phosphorylating c-Myc, which is critical for its stability (72).

The docking of DH_22 on the mTOR kinase domain of mTORC2 (Figure 5) provided a good affinity, with binding affinity around -7.610 kcal/mol. The compound also interacts quite nice with one of the ATP-binding residues, Lys2187, through conventional Hydrogen Bond with reasonable distance at 2.65 Å (73). This result indicates that DH_22 could inhibit mTOR through ATP-competitive manner. However, it is worth to note that the interaction lack of stacking with residue Trp2239 that was often found in the interaction of mTOR ATP-competitive inhibitor such as Torin2 or PP242. In addition, interaction with Leu2185 indicates the occupation of the N-lobe pocket of mTOR kinase by DH_22 (74).

Meanwhile, for the docking on Akt1, the ligand-protein binding interaction was calculated at -8.389 kcal/mol. This energy was much more negative compared to the previous interaction; thus, it is predicted that the interaction between DH_22 and Akt1 was stronger than with mTOR of mTORC2. In addition,

there were four hydrogen bonds, even though in the type of non-classical hydrogen bond, in the interaction of DH_22 with Akt1. However, the observed compound was not interacting with residue Trp80 of Akt1 with π - π stacking interaction, which is one of the key interactions in the allosteric inhibition of Akt (75).

Table 1. Docking results of DH_22.

Macromolecules	Binding Affinity (kcal/mol)		Interacting residue(s)			
	DH_22	Native	Conventional Bond	HNon-Classical bonds	H Electrostatic	π Hydrophobic
mTOR kinase domain of mTORC2 (PDB ID 4JT5)	-7.610	-8.893 (inhibitor: pp242)	Lys2187 (2.65 Å)	Cys2243 (3.43 Å), Ser2342 (3.42 Å)	N/A	Leu2185, Tyr2225, Ile2237, Ile2356
Akt1 (*)	-8.389	-14.289 (inhibitor:16a)	Asn54 (3.02 Å), Cys296(3.38 Å)	Glu17 (3.80 Å), Tyr18 (3.42 Å), Thr82 (4.03 Å), Tyr326 (3.57 Å)	Arg273	Tyr18, Cys296

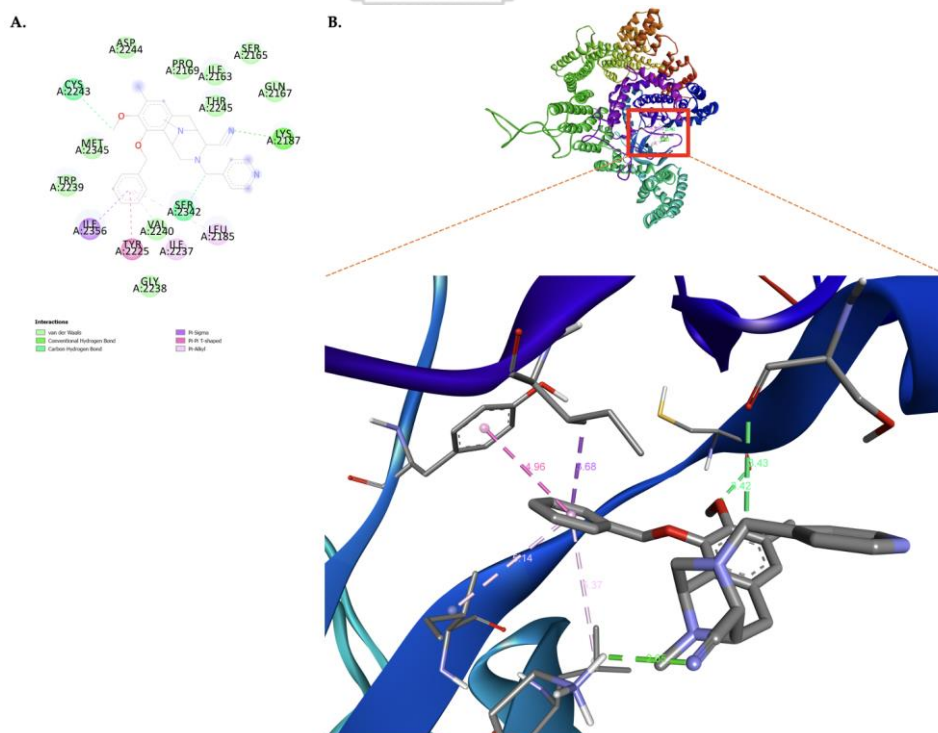


Figure 13. Docking results of DH_22 on mTOR kinase domain of mTORC2 (PDB ID 4JT5).

(A) 2D diagram interaction of DH_22 with mTOR kinase domain of mTORC2 residues. (B) 3D picture of DH_22 with mTOR kinase domain of mTORC2.

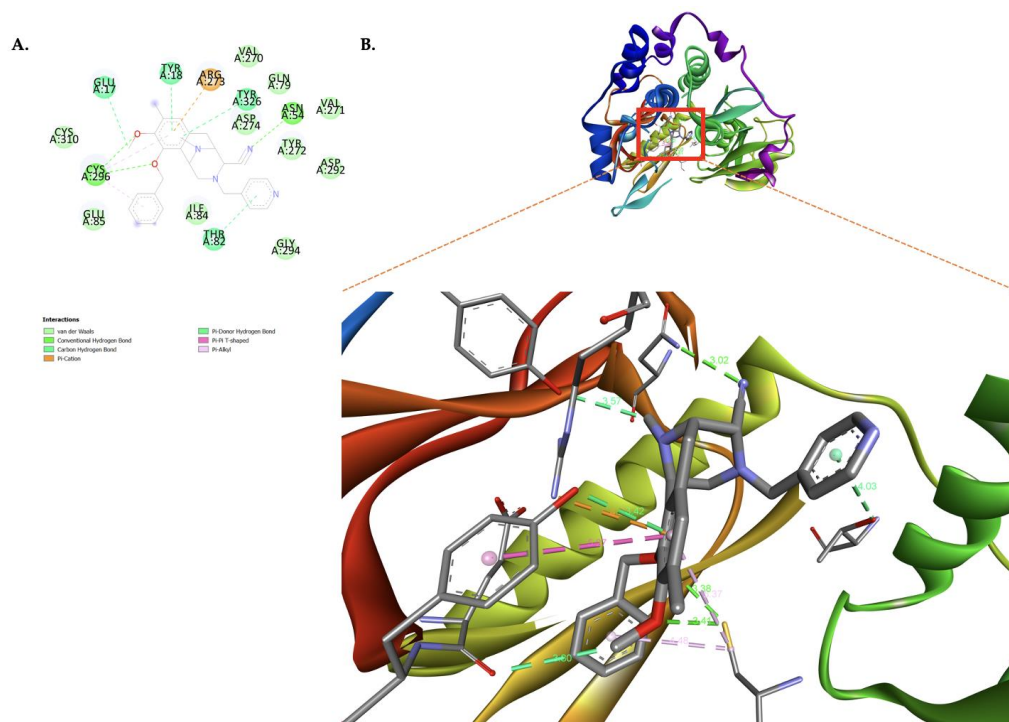


Figure 14. Docking results of DH-22 on Akt1 (PDB ID 6S9W).

(A) 2D diagram interaction of DH-22 with Akt1. (B) 3D picture of DH_22 on the Akt1 kinase domain.

CHAPTER V

DISCUSSION AND CONCLUSION

The RT derivative DH_22 (Figure 6) is a novel compound synthesized based on the right-half structure of RT, or RM-based hybrid renieramycin-ecteinascidin derivative (28), which was isolated from the Thai blue sponge *Xestopongia sp.* We synthesized various derivatives of renieramycin from marine natural products as starting materials (76) and evaluated their biological activities. The results indicated that a compound was effective when aromatic rings (especially pyridine rings) were introduced in place of the angelate in the C-1 substituent of renieramycins (77, 78). The substituent at N-3 of the tricyclic skeleton corresponds to the right half of renieramycin and is expected to affect the C-1 side chain of renieramycins. Thus, the pyridine-4-ylmethyl group of DH-22 was introduced with the expectation of acting as a pyridine ring of the C-1 side chain of the renieramycin derivative.

Our study found that DH-22 has a cytotoxic effect on human A549 cells with an IC_{50} value of $13.27 \pm 0.66 \mu\text{M}$ (Figure 7A). Subsequently, Annexin V/PI staining indicated that the elimination of cancer cells occurred through apoptosis (Figure 7B and C). Annexin V/PI staining, used for detecting both apoptotic and necrotic cells, relies on the ability of Annexin V to bind to phosphatidylserine, which is normally located on the inner leaflet of the plasma membrane but is exposed on the outer leaflet during apoptosis (79, 80). Annexin V-positive and PI-negative cells are considered to be in early-stage apoptosis, while Annexin V-positive and PI-positive cells are considered to be in late-stage apoptosis (81).

Based on its simple structure, DH_22 has effectiveness in cytotoxicity effects on lung cancer when compared to some other renieramycin derivatives. Suksamai in her research stated that the IC_{50} of her compound 5-O-(N-Boc-L-Alanine)-Renieramycin T is $7 \mu\text{M}$ (82), and Hongwiangchan with his compound Hydroquinone 5-O-Cinnamoyl Ester of Renieramycin M has an IC_{50} of $14 \mu\text{M}$ (22), both of which have the structure which is very complex even bigger than the structure of the starting

material. Tests on other methods also showed effectiveness which shows they can inhibit the growth of cancer cells.

Additionally, morphological characteristics of apoptosis-related cytotoxicity were observed in cells treated with DH-22 (Figure 8A and B). Apoptotic cells typically appear bright with condensed nuclei and fragmented or condensed chromatin when stained with Hoechst. In contrast, necrotic cells appear swollen with irregularly shaped nuclei and dispersed chromatin (83, 84). Necrotic cells may also have cytoplasmic vacuolation or ruptured plasma membranes (85).

Apoptosis is the outcome of a cascade of molecular processes resulting in caspase activation and substrate cleavage. Caspases are cysteine proteases involved in the beginning and end of apoptosis. Caspase-9 is an initiator caspase that is activated in response to pro-apoptotic signals by the release of cytochrome c from the mitochondria. Caspase-9, once activated, cleaves and activates downstream effector caspases, such as caspase-3, resulting in the destruction of cellular components and cell death (86).

PARP, a nuclear enzyme involved in DNA repair, is one of the essential substrates of effector caspases. PARP cleavage by active caspases results in the loss of its enzymatic activity and the buildup of PARP cleavage fragments, which indicates that apoptosis is still occurring. The biochemical activities caused by caspase activation and PARP cleavage are also in line with the morphological alterations observed during apoptosis (Figure 8C and D).

The p53-dependent pathway, a key apoptotic pathway, was found to be activated by DH-22 treatment. The tumor suppressor protein p53 is involved in DNA repair, cell cycle arrest, and apoptotic cell death. It is activated in response to DNA damage by ataxia telangiectasia-mutated kinases (87). The activation of p53 alters the cellular balance of Bcl-2 family proteins, increasing the levels pro-apoptotic protein (Bax) while decreasing those of anti-apoptotic protein (Bcl-2) (Figure 9). The concurrent apoptotic effect was mediated via intrinsic mode through the up-regulation of Bax and activated cleaved caspase-9, as well as the down-regulation of Bcl-2 and full-length caspase-9 expression (88). The death-survival threshold is then modified by the competitive dimerization of pro- and anti-apoptotic proteins. The

pro-apoptotic dimers may induce the release of mitochondrial contents into the cytoplasm, which activate caspase-9 (89). This process leads to the activation of PARP to avoid the depletion of energy (NAD and ATP), which is necessary for the later stages of apoptosis (90).

Further research is required to determine the ability of DH_22 to inhibit cell proliferation. MTT was served as initial test for proliferation. These findings suggested that DH_22 compound has a significant and time-dependent influence on cancer cell viability. The considerable reduction in cell viability and metabolic activity seen at each time point showed that DH_22 inhibits cancer cell growth and produces cell death. This highlighted the compound's potential as a promising anti-cancer drug. Furthermore, the findings from the clonogenic assay align with the previous results indicating that DH_22 gave strong evidence of efficiency in preventing cancer cell proliferation (Figure 10). The assay found that the compound-treated group had significantly zero colony development than the control group.

In order to obtain a better knowledge, mechanistic investigations are required to elucidate the molecular processes behind the compound's inhibitory effects on cell development. This might include looking at how the chemical therapy affects certain signaling pathways, gene expression patterns, or protein interactions. Akt is normally in charge of the genes that promote cell development. The activation of Akt pathways in lung cancer transcription factors was found to operate in an upstream regulatory mechanism (91). The activation of PI3k/Akt signaling pathways triggers the overexpression of c-Myc, whereas Akt seems to stabilize it, as reported in several past studies (92). Myc is a leucine zipper transcription factor with a basic helix-loop-helix structure that regulates various target genes involved in cell development, metabolism, differentiation, proliferation, and apoptosis (93).

GSK3 β is one of the factors that can induce the degradation of c-Myc (Figure 7). When GSK3 β is active, it can phosphorylate c-Myc at two specific sites, Thr58 and Ser62, which leads to ubiquitination and degradation of c-Myc. This process is facilitated by the E3 ubiquitin ligase complex, which recognizes and tags phosphorylated c-Myc for degradation by the proteasome (94, 95). Akt regulates c-

Myc stability by inhibiting GSK3 β , protecting it against proteasomal degradation (67). Therefore, interfering with the Akt signal will destabilize c-Myc, significantly suppressing cancer cells.

AutoDock Vina was used to carry out molecular docking, it used a scoring function called the binding affinity to predict the strength of binding between a ligand and a target protein. The binding affinity is typically expressed as a negative value, where more negative values indicate stronger binding. Additionally, in AutoDock Vina, a binding affinity score below 0 is generally considered favorable, with more negative scores indicating stronger binding. The exact range of “good” binding affinity can vary depending on the specific system and context. However, in general, a binding affinity score of -5 kcal/mol or lower is often considered as a good binding affinity (96, 97).

The result stated that DH_22 can inhibit both mTOR via the ATP-competitive mode with binding affinity was -7.610 kcal/mol, and Akt was -8.389 kcal/mol, via the allosteric mode. The phosphorylation of Akt1 by mTOR, particularly mTORC2, indicates its full activation, which could inhibit GSK3 β by phosphorylating its Ser6 residue (98, 99). As mentioned previously, GSK3 β stabilizes c-Myc by initiating its ubiquitination. The molecular docking study indicates that DH_22 alters the stability of c-Myc by inhibiting the upstream protein. The inhibition of mTORC2 will reduce the phosphorylation of Akt, reducing the phosphorylation of GSK3 β and degrading c-Myc. In addition, DH_22 itself could inhibit Akt via the allosteric mode, which could disrupt the c-Myc stabilization pathway. Owing to its dual-inhibition mechanism, DH_22 is a promising candidate for c-Myc-induced cancer drugs with mTOR mutation.

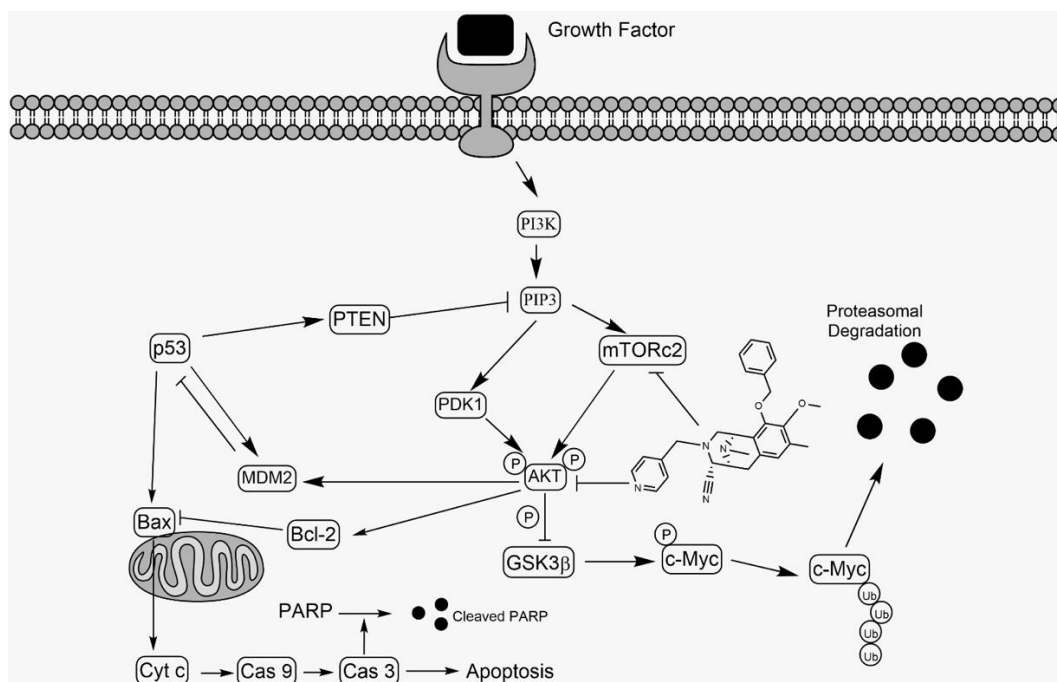


Figure 15. Proposed mechanism of action of DH₂₂.

In conclusion, DH₂₂ is a novel compound synthesized from marine natural products that has been shown to efficiently induce apoptosis in cancer cells. DH-22 treatment resulted in cytotoxicity with an IC₅₀ value of $13.27 \pm 0.66 \mu\text{M}$ in human A549 cells. Apoptosis was confirmed through Annexin V/PI staining and cell morphology observation. DH-22 induced apoptosis through the up-regulation of p53, Bax, cleaved caspase-9, and cleaved PARP, as well as the down-regulation of Bcl-2 expression. According to the findings of this investigation, DH-22 has a high potential for further development as a novel medicine. Furthermore, DH₂₂ has a good ability to inhibit lung cancer proliferation by inhibiting the Akt/c-Myc signaling pathway. The mechanism of action starts with the inhibition of mTORC2, which will reduce the phosphorylation of Akt and consecutively reduce the phosphorylation of GSK3 β and degrade c-Myc. In addition, DH₂₂ itself could inhibit Akt via the allosteric mode, which could destabilize c-Myc. The results of this study suggest advancing DH₂₂ as a potential new therapy for lung cancer.

REFERENCES



จุฬาลงกรณ์มหาวิทยาลัย
CHULALONGKORN UNIVERSITY

1. Sung H, Ferlay J, Siegel RL, Laversanne M, Soerjomataram I, Jemal A, et al. Global Cancer Statistics 2020: GLOBOCAN Estimates of Incidence and Mortality Worldwide for 36 Cancers in 185 Countries. *CA: A Cancer Journal for Clinicians*. 2021;71(3):209-49.
2. Hanahan D, Weinberg RA. Hallmarks of cancer: the next generation. *Cell*. 2011;144(5):646-74.
3. Pfeffer CM, Singh ATK. Apoptosis: A Target for Anticancer Therapy. *Int J Mol Sci*. 2018;19(2).
4. Kasibhatla S, Tseng B. Why Target Apoptosis in Cancer Treatment? *Molecular Cancer Therapeutics*. 2003;2(6):573-80.
5. Papaliagkas V, Anogianaki A, Anogianakis G, Ilonidis G. The proteins and the mechanisms of apoptosis: a mini-review of the fundamentals. *Hippokratia*. 2007;11(3):108-13.
6. Jiang X, Wang X. Cytochrome C-mediated apoptosis. *Annu Rev Biochem*. 2004;73:87-106.
7. Liu P, Begley M, Michowski W, Inuzuka H, Ginzberg M, Gao D, et al. Cell-cycle-regulated activation of Akt kinase by phosphorylation at its carboxyl terminus. *Nature*. 2014;508(7497):541-5.
8. Chen H, Liu H, Qing G. Targeting oncogenic Myc as a strategy for cancer treatment. *Signal Transduct Target Ther*. 2018;3:5.
9. Fan Y, Dickman KG, Zong W-X. Akt and c-Myc differentially activate cellular metabolic programs and prime cells to bioenergetic inhibition. *The Journal of biological chemistry*. 2010;285(10):7324-33.
10. Nitulescu GM, Van De Venter M, Nitulescu G, Ungurianu A, Juzenas P, Peng Q, et al. The Akt pathway in oncology therapy and beyond (Review). *Int J Oncol*. 2018;53(6):2319-31.
11. Li Q, Li S, Yang X, Zhang X, Song C, Zhu S. Association between RNF2+P-AKT expression in pretreatment biopsy specimens, and poor survival following radiotherapy in patients with esophageal squamous cell carcinoma. *Oncol Lett*. 2019;18(4):3734-42.

12. Chiappini PBO, de Medeiros IUD, Lima LGC, Fregnani JH, Nonogaki S, da Costa WL, Jr., et al. Prognostic implications of phosphatidylinositol 3-kinase/AKT signaling pathway activation in gastric carcinomas. *Arch Med Sci.* 2017;13(6):1262-8.
13. Wang X, Wang X, Xu Y, Yan M, Li W, Chen J, et al. Effect of nicastrin on hepatocellular carcinoma proliferation and apoptosis through PI3K/AKT signalling pathway modulation. *Cancer Cell Int.* 2020;20:91.
14. Liu W, Wang Q, Li F, Zhang S, Cao L. [Correlations between the p-Akt-mTOR-p70S6K pathway and clinicopathological features or chemoresistance of ovarian cancer]. *Zhong Nan Da Xue Xue Bao Yi Xue Ban.* 2017;42(8):882-8.
15. Lu J, Zang H, Zheng H, Zhan Y, Yang Y, Zhang Y, et al. Overexpression of p-Akt, p-mTOR and p-eIF4E proteins associates with metastasis and unfavorable prognosis in non-small cell lung cancer. *PLoS One.* 2020;15(2):e0227768.
16. Zheng H, Zhan Y, Zhang Y, Liu S, Lu J, Yang Y, et al. Elevated expression of G3BP1 associates with YB1 and p-AKT and predicts poor prognosis in nonsmall cell lung cancer patients after surgical resection. *Cancer Med.* 2019;8(16):6894-903.
17. Kitano H, Chung JY, Ylaya K, Conway C, Takikita M, Fukuoka J, et al. Profiling of phospho-AKT, phospho-mTOR, phospho-MAPK and EGFR in non-small cell lung cancer. *J Histochem Cytochem.* 2014;62(5):335-46.
18. Hu J, Liu YL, Piao SL, Yang DD, Yang YM, Cai L. Expression patterns of USP22 and potential targets BMI-1, PTEN, p-AKT in non-small-cell lung cancer. *Lung Cancer.* 2012;77(3):593-9.
19. Hu ZY, Huang WY, Zhang L, Huang B, Chen SC, Li XL. Expression of AKT and p-AKT protein in lung adenocarcinoma and its correlation with PD-L1 protein and prognosis. *Ann Transl Med.* 2020;8(18):1172.
20. Miller DM, Thomas SD, Islam A, Muench D, Sedoris K. c-Myc and cancer metabolism. *Clin Cancer Res.* 2012;18(20):5546-53.
21. Elbadawy M, Usui T, Yamawaki H, Sasaki K. Emerging Roles of C-Myc in Cancer Stem Cell-Related Signaling and Resistance to Cancer Chemotherapy: A Potential Therapeutic Target Against Colorectal Cancer. *Int J Mol Sci.* 2019;20(9).

22. Hongwiangchan N, Sriratanasak N, Wichadakul D, Aksorn N, Chamni S, Chanvorachote P. Hydroquinone 5-O-Cinnamoyl Ester of Renieramycin M Suppresses Lung Cancer Stem Cells by Targeting Akt and Destabilizes c-Myc. *Pharmaceuticals (Basel)*. 2021;14(11).
23. Fagnocchi L, Zippo A. Multiple Roles of MYC in Integrating Regulatory Networks of Pluripotent Stem Cells. *Front Cell Dev Biol*. 2017;5:7.
24. Chanvorachote P, Sriratanasak N, Nonpanya N. C-myc Contributes to Malignancy of Lung Cancer: A Potential Anticancer Drug Target. *Anticancer Res*. 2020;40(2):609-18.
25. Segrelles C, Moral M, Lara M, Ruiz Macias S, Santos M, Leis H, et al. Molecular determinants of Akt-induced keratinocyte transformation. *Oncogene*. 2006;25:1174-85.
26. Stengel S, Petrie KR, Sbirkov Y, Stanko C, Ghazvini Zadeegan F, Gil V, et al. Suppression of MYC by PI3K/AKT/mTOR pathway inhibition in combination with all-trans retinoic acid treatment for therapeutic gain in acute myeloid leukaemia. *British Journal of Haematology*. 2022;198(2):338-48.
27. Molinski TF, Dalisay DS, Lievens SL, Saludes JP. Drug development from marine natural products. *Nature Reviews Drug Discovery*. 2009;8(1):69-85.
28. Daikuhara N, Tada Y, Yamaki S, Charupant K, Amnuoypol S, Suwanborirux K, et al. Chemistry of renieramycins. Part 7: Renieramycins T and U, novel renieramycin–ecteinascidin hybrid marine natural products from Thai sponge *Xestospongia* sp. *Tetrahedron Letters*. 2009;50(29):4276-8.
29. Yokoya M, Toyoshima R, Suzuki T, Le VH, Williams RM, Saito N. Stereoselective Total Synthesis of (–)-Renieramycin T. *The Journal of Organic Chemistry*. 2016;81(10):4039-47.
30. Chamni S, Sirimangkalakitti N, Chanvorachote P, Saito N, Suwanborirux K. Chemistry of Renieramycins. 17. A New Generation of Renieramycins: Hydroquinone 5-O-Monoester Analogues of Renieramycin M as Potential Cytotoxic Agents against Non-Small-Cell Lung Cancer Cells. *J Nat Prod*. 2017;80(5):1541-7.

31. Ranu BC, Jana R, Sowmiah S. An improved procedure for the three-component synthesis of highly substituted pyridines using ionic liquid. *J Org Chem.* 2007;72(8):3152-4.
32. Jemmezi F, Kether F, Ismail A, Jamoussi B, Khiari J. Synthesis and biological activity of novel benzothiazole pyridine derivatives. *IOSR Journal of Applied Chemistry.* 2014;7:62-4.
33. Sahu R, Mishra R, Kumar R, Salahuddin, Majee C, Mazumder A, et al. Pyridine Moiety: An Insight into Recent Advances in the Treatment of Cancer. *Mini Rev Med Chem.* 2022;22(2):248-72.
34. Yoshio H. Role of Pyridines in Medicinal Chemistry and Design of BACE1 Inhibitors Possessing a Pyridine Scaffold. In: Pratima Parashar P, editor. *Pyridine.* Rijeka: IntechOpen; 2018. p. Ch. 2.
35. Muangnoi C, Ratnatilaka Na Bhuket P, Jithavech P, Wichitnithad W, Srikun O, Nerungsi C, et al. Scale-Up Synthesis and In Vivo Anti-Tumor Activity of Curcumin Diethyl Disuccinate, an Ester Prodrug of Curcumin, in HepG2-Xenograft Mice. *Pharmaceutics.* 2019;11(8).
36. Perez-Warnisher MT, De Miguel M, Seijo LM. Tobacco Use Worldwide: Legislative Efforts to Curb Consumption. *Ann Glob Health.* 2018;84(4):571-9.
37. Xing PY, Zhu YX, Wang L, Hui ZG, Liu SM, Ren JS, et al. What are the clinical symptoms and physical signs for non-small cell lung cancer before diagnosis is made? A nation-wide multicenter 10-year retrospective study in China. *Cancer Med.* 2019;8(8):4055-69.
38. Yount S, Beaumont J, Rosenbloom S, Cella D, Patel J, Hensing T, et al. A brief symptom index for advanced lung cancer. *Clin Lung Cancer.* 2012;13(1):14-23.
39. Sharma R. Mapping of global, regional and national incidence, mortality and mortality-to-incidence ratio of lung cancer in 2020 and 2050. *Int J Clin Oncol.* 2022;27(4):665-75.
40. Schabath MB, Cote ML. Cancer Progress and Priorities: Lung Cancer. *Cancer Epidemiol Biomarkers Prev.* 2019;28(10):1563-79.
41. Bossé Y, Amos CI. A Decade of GWAS Results in Lung Cancer. *Cancer Epidemiol Biomarkers Prev.* 2018;27(4):363-79.

42. Dela Cruz CS, Tanoue LT, Matthay RA. Lung cancer: epidemiology, etiology, and prevention. *Clin Chest Med.* 2011;32(4):605-44.
43. Mehta A, Dobersch S, Romero-Olmedo AJ, Barreto G. Epigenetics in lung cancer diagnosis and therapy. *Cancer Metastasis Rev.* 2015;34(2):229-41.
44. Cersosimo R. Lung cancer: A review. *American journal of health-system pharmacy : AJHP : official journal of the American Society of Health-System Pharmacists.* 2002;59:611-42.
45. Purandare NC, Rangarajan V. Imaging of lung cancer: Implications on staging and management. *Indian J Radiol Imaging.* 2015;25(2):109-20.
46. Howington JA, Blum MG, Chang AC, Balekian AA, Murthy SC. Treatment of stage I and II non-small cell lung cancer: Diagnosis and management of lung cancer, 3rd ed: American College of Chest Physicians evidence-based clinical practice guidelines. *Chest.* 2013;143(5 Suppl):e278S-e313S.
47. Chemotherapy in non-small cell lung cancer: a meta-analysis using updated data on individual patients from 52 randomised clinical trials. Non-small Cell Lung Cancer Collaborative Group. *Bmj.* 1995;311(7010):899-909.
48. Ramalingam S, Belani C. Systemic chemotherapy for advanced non-small cell lung cancer: recent advances and future directions. *Oncologist.* 2008;13 Suppl 1:5-13.
49. Amini A, Yeh N, Gaspar LE, Kavanagh B, Karam SD. Stereotactic body radiation therapy (SBRT) for lung cancer patients previously treated with conventional radiotherapy: a review. *Radiat Oncol.* 2014;9:210.
50. Zappa C, Mousa SA. Non-small cell lung cancer: current treatment and future advances. *Translational Lung Cancer Research.* 2016;5(3):288-300.
51. Tang D, Kang R, Berghe TV, Vandenabeele P, Kroemer G. The molecular machinery of regulated cell death. *Cell Research.* 2019;29(5):347-64.
52. Goldar S, Khaniani MS, Derakhshan SM, Baradaran B. Molecular mechanisms of apoptosis and roles in cancer development and treatment. *Asian Pac J Cancer Prev.* 2015;16(6):2129-44.
53. Jan R, Chaudhry GE. Understanding Apoptosis and Apoptotic Pathways Targeted Cancer Therapeutics. *Adv Pharm Bull.* 2019;9(2):205-18.

54. Creative Diagnostic. Intrinsic Apoptosis Pathway [cited 2022 15 October]. Available from: <https://www.creative-diagnostics.com/intrinsic-apoptosis-pathway.htm>.
55. Ghobrial IM, Witzig TE, Adjei AA. Targeting apoptosis pathways in cancer therapy. *CA Cancer J Clin*. 2005;55(3):178-94.
56. Datta SR, Brunet A, Greenberg ME. Cellular survival: a play in three Akts. *Genes Dev*. 1999;13(22):2905-27.
57. Chuang CH, Cheng TC, Leu YL, Chuang KH, Tzou SC, Chen CS. Discovery of Akt kinase inhibitors through structure-based virtual screening and their evaluation as potential anticancer agents. *Int J Mol Sci*. 2015;16(2):3202-12.
58. Al-Bazz YO, Underwood JC, Brown BL, Dobson PR. Prognostic significance of Akt, phospho-Akt and BAD expression in primary breast cancer. *Eur J Cancer*. 2009;45(4):694-704.
59. Song M, Bode AM, Dong Z, Lee M-H. AKT as a Therapeutic Target for Cancer. *Cancer Research*. 2019;79(6):1019-31.
60. Vadlakonda L, Dash A, Pasupuleti M, Anil Kumar K, Reddanna P. The Paradox of Akt-mTOR Interactions. *Front Oncol*. 2013;3:165.
61. Yang Y, Luo J, Zhai X, Fu Z, Tang Z, Liu L, et al. Prognostic value of phospho-Akt in patients with non-small cell lung carcinoma: a meta-analysis. *Int J Cancer*. 2014;135(6):1417-24.
62. Jia W, Chang B, Sun L, Zhu H, Pang L, Tao L, et al. REDD1 and p-AKT over-expression may predict poor prognosis in ovarian cancer. *Int J Clin Exp Pathol*. 2014;7(9):5940-9.
63. Song M, Bode AM, Dong Z, Lee MH. AKT as a Therapeutic Target for Cancer. *Cancer Res*. 2019;79(6):1019-31.
64. Yao Z, Gao G, Yang J, Long Y, Wang Z, Hu W, et al. Prognostic Role of the Activated p-AKT Molecule in Various Hematologic Malignancies and Solid Tumors: A Meta-Analysis. *Frontiers in Oncology*. 2020;10.
65. Murphy MJ, Wilson A, Trumpp A. More than just proliferation: Myc function in stem cells. *Trends Cell Biol*. 2005;15(3):128-37.

66. Creative Diagnostic. C-MYC Signaling Pathway [cited 2022 15 October]. Available from: <https://www.creative-diagnostics.com/c-myc-signaling-pathway.htm>.
67. Swords RT, Schenk T, Stengel S, Gil VS, Petrie KR, Perez A, et al. Inhibition of the PI3K/AKT/mTOR Pathway Leads to Down-Regulation of c-Myc and Overcomes Resistance to ATRA in Acute Myeloid Leukemia. *Blood*. 2015;126(23):1363.
68. Madden SK, de Araujo AD, Gerhardt M, Fairlie DP, Mason JM. Taking the Myc out of cancer: toward therapeutic strategies to directly inhibit c-Myc. *Molecular Cancer*. 2021;20(1):3.
69. Gabay M, Li Y, Felsher DW. MYC activation is a hallmark of cancer initiation and maintenance. *Cold Spring Harb Perspect Med*. 2014;4(6).
70. Farrell AS, Sears RC. MYC degradation. *Cold Spring Harb Perspect Med*. 2014;4(3).
71. Matsubara T, Yokoya M, Sirimangkalakitti N, Saito N. Asymmetric Synthesis and Cytotoxicity Evaluation of Right-Half Models of Antitumor Renieramycin Marine Natural Products. *Mar Drugs*. 2018;17(1).
72. Li S, Jiang C, Pan J, Wang X, Jin J, Zhao L, et al. Regulation of c-Myc protein stability by proteasome activator REGgamma. *Cell Death Differ*. 2015;22(6):1000-11.
73. Stary D, Nepovimova E, Kuca K, Bajda M. Searching for new mTOR kinase inhibitors: Analysis of binding sites and validation of docking protocols. *Chem Biol Drug Des*. 2023;101(1):103-19.
74. Yang H, Rudge DG, Koos JD, Vaidialingam B, Yang HJ, Pavletich NP. mTOR kinase structure, mechanism and regulation. *Nature*. 2013;497(7448):217-23.
75. Quambusch L, Landel I, Depta L, Weisner J, Uhlenbrock N, Muller MP, et al. Covalent-Allosteric Inhibitors to Achieve Akt Isoform-Selectivity. *Angew Chem Int Ed Engl*. 2019;58(52):18823-9.
76. Petsri K, Yokoya M, Racha S, Thongsom S, Thepthanee C, Innets B, et al. Novel Synthetic Derivative of Renieramycin T Right-Half Analog Induces Apoptosis and Inhibits Cancer Stem Cells via Targeting the Akt Signal in Lung Cancer Cells. *Int J Mol Sci*. 2023;24(6).
77. Charupant K, Daikuhara N, Saito E, Amnuoyopol S, Suwanborirux K, Owa T, et al. Chemistry of renieramycins. Part 8: synthesis and cytotoxicity evaluation of

- renieramycin M-jorunnamycin A analogues. *Bioorg Med Chem*. 2009;17(13):4548-58.
78. Charupant K, Suwanborirux K, Daikuhara N, Yokoya M, Ushijima-Sugano R, Kawai T, et al. Microarray-based transcriptional profiling of renieramycin M and jorunnamycin C, isolated from Thai marine organisms. *Mar Drugs*. 2009;7(4):483-94.
79. Crowley LC, Marfell BJ, Scott AP, Waterhouse NJ. Quantitation of Apoptosis and Necrosis by Annexin V Binding, Propidium Iodide Uptake, and Flow Cytometry. *Cold Spring Harb Protoc*. 2016;2016(11).
80. van Engeland M, Nieland LJ, Ramaekers FC, Schutte B, Reutelingsperger CP. Annexin V-affinity assay: a review on an apoptosis detection system based on phosphatidylserine exposure. *Cytometry*. 1998;31(1):1-9.
81. Brauchle E, Thude S, Brucker SY, Schenke-Layland K. Cell death stages in single apoptotic and necrotic cells monitored by Raman microspectroscopy. *Scientific Reports*. 2014;4(1):4698.
82. Suksamai D, Racha S, Sriratanasak N, Chaotham C, Aphicho K, Lin ACK, et al. 5-O-(N-Boc-L-Alanine)-Renieramycin T Induces Cancer Stem Cell Apoptosis via Targeting Akt Signaling. *Mar Drugs*. 2022;20(4).
83. Plesca D, Mazumder S, Almasan A. DNA damage response and apoptosis. *Methods Enzymol*. 2008;446:107-22.
84. Frankfurt OS, Krishan A. Identification of apoptotic cells by formamide-induced dna denaturation in condensed chromatin. *J Histochem Cytochem*. 2001;49(3):369-78.
85. Golstein P, Kroemer G. Cell death by necrosis: towards a molecular definition. *Trends in Biochemical Sciences*. 2007;32(1):37-43.
86. Saraste A, Pulkki K. Morphologic and biochemical hallmarks of apoptosis. *Cardiovasc Res*. 2000;45(3):528-37.
87. Blackford AN, Jackson SP. ATM, ATR, and DNA-PK: The Trinity at the Heart of the DNA Damage Response. *Mol Cell*. 2017;66(6):801-17.
88. Chimplee S, Roytrakul S, Sukrong S, Srisawat T, Graidist P, Kanokwiroon K. Anticancer Effects and Molecular Action of 7-alpha-Hydroxyfrullanolide in G2/M-

- Phase Arrest and Apoptosis in Triple Negative Breast Cancer Cells. *Molecules*. 2022;27(2).
89. Garrido C, Galluzzi L, Brunet M, Puig PE, Didelot C, Kroemer G. Mechanisms of cytochrome c release from mitochondria. *Cell Death & Differentiation*. 2006;13(9):1423-33.
90. Boulares AH, Yakovlev AG, Ivanova V, Stoica BA, Wang G, Iyer S, et al. Role of poly(ADP-ribose) polymerase (PARP) cleavage in apoptosis. Caspase 3-resistant PARP mutant increases rates of apoptosis in transfected cells. *J Biol Chem*. 1999;274(33):22932-40.
91. Iksen, Pothongsrisit S, Pongrakhananon V. Targeting the PI3K/AKT/mTOR Signaling Pathway in Lung Cancer: An Update Regarding Potential Drugs and Natural Products. *Molecules*. 2021;26(13).
92. Hartl M. The Quest for Targets Executing MYC-Dependent Cell Transformation. *Frontiers in Oncology*. 2016;6.
93. Padmanabhan A, Li X, Bieberich CJ. Protein kinase A regulates MYC protein through transcriptional and post-translational mechanisms in a catalytic subunit isoform-specific manner. *J Biol Chem*. 2013;288(20):14158-69.
94. Gregory MA, Qi Y, Hann SR. Phosphorylation by glycogen synthase kinase-3 controls c-myc proteolysis and subnuclear localization. *J Biol Chem*. 2003;278(51):51606-12.
95. Duda P, Akula SM, Abrams SL, Steelman LS, Martelli AM, Cocco L, et al. Targeting GSK3 and Associated Signaling Pathways Involved in Cancer. *Cells*. 2020;9(5).
96. Gaillard T. Evaluation of AutoDock and AutoDock Vina on the CASF-2013 Benchmark. *Journal of Chemical Information and Modeling*. 2018;58(8):1697-706.
97. Nguyen NT, Nguyen TH, Pham TNH, Huy NT, Bay MV, Pham MQ, et al. Autodock Vina Adopts More Accurate Binding Poses but Autodock4 Forms Better Binding Affinity. *Journal of Chemical Information and Modeling*. 2020;60(1):204-11.
98. Baffi TR, Lorden G, Wozniak JM, Feichtner A, Yeung W, Kornev AP, et al. mTORC2 controls the activity of PKC and Akt by phosphorylating a conserved TOR interaction motif. *Sci Signal*. 2021;14(678).

99. Hermida MA, Dinesh Kumar J, Leslie NR. GSK3 and its interactions with the PI3K/AKT/mTOR signalling network. *Adv Biol Regul.* 2017;65:5-15.



VITA

NAME Indiana Gita Anggraeni

DATE OF BIRTH 09 August 1996

PLACE OF BIRTH Demak

INSTITUTIONS ATTENDED University of Darussalam Gontor

HOME ADDRESS Bumi Wonosalam Asri Regency No.36 Jogoloyo, Wonosalam,
Demak, Central Java, Indonesia 59571

